WIRELESS INTERNET SERVICE PROVIDING FOR 5G WITH HYBRID TV BROADCAST AND VISIBLE LIGHT COMMUNICATIONS

A Thesis

by

Sezgin Şencan

Submitted to the
Graduate School of Sciences and Engineering
In Partial Fulfillment of the Requirements for
the Degree of

Master of Science

in the
Department of Electrical and Electronics Engineering

Özyeğin University
January 2018

WIRELESS INTERNET SERVICE PROVIDING FOR 5G WITH HYBRID TV BROADCAST AND VISIBLE LIGHT COMMUNICATIONS

Approved by:

Asst. Professor Burhan Gülbahar, Advisor
Department of Electrical and Electronics Engineering
Özyeğin University

Asst. Professor Bilge Kartal Çetin
Department of Electrical and Electronics Engineering
Ege University

Professor Murat Uysal
Department of Electrical and Electronics Engineering
Özyeğin University

Date Approved: 29 December 2017

To my family

ABSTRACT

Visible light communications (VLC) is a future promising communication technology to be utilized in future 5G networks satisfying energy efficient outdoor and indoor communications with existing hardware components such as LED bulbs, TV screens and camera receivers. Existing outdoor VLC architectures have significant challenges in terms of data rate, robustness to outdoor channel and requirements of high power transmitter resources. In this thesis, a cellular outdoor VLC architecture is introduced by utilizing arrays of LED bulbs as transmitters and telescopic cameras as receivers. The proposed system promises high performance cellular uplink communication channel reaching hundreds of Kbps for the ranges of tens of kilometers. It exploits array transmitters consuming less than hundred Watts power consumption at each house and telescopes improving the communication range. Besides that, the proposed system architecture is combined with existing TV downlink radio frequency (RF) network architecture to realize internet service providing (ISP) system with low cost and low complexity system design. Networking architecture utilizes commercially available display screens at home for downlink data. Performance analysis and comparison of various next generation display technologies such as quantum dot (QD) and organic light emitting diode (OLED) based displays are performed in terms of response time, color gamut, spectral color output, contrast ratio and power consumption. VLC-RF hybrid architecture promises widespread utilization of ISP services in suburban areas with high reliability, low cost and energy efficient system design utilizing already available hardware platforms.

ÖZETÇE

Görünür ışıkla haberleşme potansiyel olarak 5G ağ yapılarında faydalanmak üzere, hem kapalı hem de açık ortamlarda enerji verimliliği yüksek yapısı ve hali hazırda var olan LED aydınlatma, TV ekranları ve kamera alıcıları gibi donanım komponentleri ile gelecek vaad etmektedir. Fakat varolan VLC mimarilerinin data hızı, açık ortamdaki kanal dayanıklılığı ve yüksek güç iletici kaynakları anlamında gelişmesi gereken noktaları vardır. Bu tez çalışmamızda,verici tarafta LED lamba dizilerinden, alıcı tarafta teleskop kamera sisteminden faydalanılarak, açık ortam hücresel bir VLC mimarisi tanıtılmıştır. Önerilen sistem her bir ev için 100 Watt güçten daha az güç tüketimi ile LED dizilerinden faydalanarak, yüzlerce Kbps hızlarda, onlarca kilometre menzilde yüksek performans hücresel uplink haberleşme kanalı sunmaktadır. Bunun yanında, önerilen sistem mimarisi düşük maliyet ve basit tasarımı ile internet sağlamak için varolan TV downlink RF ağ mimarisi ile birleştirilmiştir. Ağ mimarisi downlink kısım için ticari olarak hazır panel ekranlarından faydalanmıştır. Quantum dot (QD), organic light emitting diode (OLED) gibi gelecek nesil panel teknolojilerinin tepkime hızı, renk uzayı, spektral renk çıktılarına, kontrast ve güç tüketim performanslarına göre kıyaslama ve performans analizleri yapılmıştır. VLC ve RF melez mimarisi, hali hazırda mevcut bulunan donanm platformları ile yüksek güvenilirlik, düşük maliyet ve enerji verimliliğini esas alan sistem tasarımı ile internet hizmeti sağlama servislerinin kırsal kesimlerde geniş şekilde yayılmasını sağlamayı hedeflemektedir.

ACKNOWLEDGEMENTS

First of all, I would like to thank my advisor Asst.Prof. Burhan Gülbahar for his continuous guadiance and support.

I am thankful to my father Akın Şencan for his moral support.

I would like to thank my company VESTEL for providing me an opportunity to get a Master Degree.

I am grateful to my collegaue, Mr. Ozgur Barutcu for his support and understanding.

I am glad to my girlfriend Büşra Keleş for her moral support.

TABLE OF CONTENTS

LIST OF TABLES

LIST OF FIGURES

TABLE I. List of abbreviations.

VLC	Visible Light Communications
RF	Radio Frequency
MIMO	Multiple Input Multiple Output
ISP	Internet Service Providing
LED	Light Emitting Diode
OLED	Organic Light Emitting Diode
CG	Color Gamut
QD	Quantum Dot
LCD	Liquid Crystal Display
UHF	Ultra High Frequency
IM	Intensity Modulation
CSK	Color Shift Keying
HD	High Definition
5G	Fifth Generation
SNR	Signal to Noise Ratio

CHAPTER I

INTRODUCTION

Visible light communications (VLC) has become most significant optical wireless communication technology alternative to radio frequency (RF) with extended use of light emitting diode (LED) light bulbs. Besides, VLC solves electromagnetic spectrum scarcity by operating between 380 nm and 750 nm. The need for high data rate and more spectrum resources is increasing each day. Existing RF outdoor communication systems suffer in terms of data rate and frequency spectrum. On the other hand, existing outdoor VLC systems need to be improved in terms of data rate and communication range. At this point, the proposed novel hybrid architecture combining both TV RF broadcast and VLC promises to create a more reliable, energy efficient and long range system designquantum dot (QD) and organic light emitting diode (OLED) based displays. In this chapter, motivations behind this thesis, contributions and organization are described.

1.1 Motivations

VLC is a future promising and high performing wireless communications technology combining both illumination and communication. VLC systems either utilize commercial LED units or display screen based transmitters by forming a practical and potential building block for future fifth generation (5G) architectures with the advantages of large unlicensed bandwidths, high data rates, lack of interference between indoor and outdoor, energy efficiency and security [1]. Most of the RF spectrum portion is occupied and limited bandwidth resources are available. Thus, hybrid systems applying both RF and VLC technologies are essential. Outdoor applications

include vehicular communications, traffic information systems and marine communications [2–6]. In [7], 5.7 km range and tens of Kbps data rate are achieved. However, telescope based outdoor cellular concept, synchronization with TV broadcast and very long ranges of communication reaching tens of kms combined with coverage for hundreds of houses are not proposed.

VLC architectures allow using the existing hardware units and infrastructures by lowering the deployment cost. Therefore, taking advantage of VLC technology developments and combining with existing TV RF broadcast signals in a hybrid downlink and uplink system to increase efficiency are the main targets in this thesis. VLC and RF hybrid networks increase system capacity and provide seamless reliable coverage [8].

In this thesis, a novel hybrid RF and VLC outdoor cellular concept is theoretically defined for Internet service providing (ISP) in developing regions. TV broadcast is merged with display screen based indoor communications for downlink channels. In the uplink, simple LED arrays on the roofs of the houses connect with camera receivers combined with high focal length telescopes creating cellular coverage areas. Besides that, developments in display technologies such as quantum dot (QD) enhancement film (QDEF), organic light emitting diode (OLED) and improved liquid crystal (LC) displays (LCDs) critically effect the VLC performance. The performance analysis achieved in terms of response time, color gamut (CG), spectral color output, static contrast ratio, power consumption and lifetime, for the first time, provides the foundations for the comparison of display screen supported VLC technologies in consumer products.

In addition, the proposed system promises to be utilized for ad hoc networks in suburban or undeveloped regions, the regions where it is difficult to establish a cable ADSL infrastructure, or in emergency situations such as earthquakes resulting in the failure of cable or wireless internet. Other communication architectures such as

satellite systems have huge latency for trip time between the satellite and the roof antenna. The weather conditions effect satellite connection more severely due to larger distance between the antenna and the satellite compared with the distance between the roof antenna/LED array and the hybrid TV/VLC broadcast station. Besides, the cabled ISP is highly costly due to cabling underground and it is impossible in some regional areas such as suburban areas. Especially, in emergency situations, cable network becomes in failure. Thus, our system becomes a good alternative in terms of both cost and safety aspects.

1.2 Contributions

The content in this thesis is published in the following work :

B. Gulbahar and S. Sencan, "Wireless Internet Service Providing for 5G with Hybrid TV Broadcast and Visible Light Communications", *Proc. of The IEEE IFIP Wireless Days (WD)*, Porto, Portugal, pp. 66-69, March 2017.

In this thesis, the contributions, achieved for the first time, are listed as follows:

- Theoretical modeling and design of a novel ISP networking infrastructure with new hybrid network architecture including uplink and downlink compatible with VLC and RF broadcast.

- VLC cellular uplink capacity and coverage analysis, numerical simulations and performance evaluations.

- Design and theoretical modeling of a long range VLC hybrid system reaching up to 50 km ranges for the first time and Kbps data rates by combining high focal length telescopes with LED arrays consuming less than hundreds of watts power.

- Theoretical comparison of indoor downlink VLC channels for display screen technologies of QD, OLED and LCD with the performance parameters including

channel capacity, probability of error, frame rate, response time, color gamut, spectral distribution and power efficiency of light radiation, contrast ratio and overall lifetime.

1.3 Organization

In Chapter II, fundamentals of VLC systems are described for VLC systems. Outdoor VLC systems are discussed in Chapter III while next generation display screen technologies in Chapter IV. In Chapter V, low cost wireless ISP arhitectures are summarized while hybrid VLC technologies are discussed in Chapter VI. Then, hybrid VLC-RF ISP infrastructure is presented in detail in Chapter VII. Numerical simulations and comparisons for the channel capacities are performed in Chapter VIII. Estimated overall system cost is calculated in Chapter IX. In Chapter X, the challenges and future research issues are discussed. Finally, in Chapter XI, the conclusions are given.

CHAPTER II

FUNDAMENTALS OF VISIBLE LIGHT COMMUNICATIONS

2.1 Introduction

VLC is the next generation optical wireless communication technology that uses commercial LED units or display screens as transmitters and photodioes or cameras as receivers. VLC utilizes visible light spectrum which is 10000 times larger than RF spectrum (from 428 to 750 THz) as shown in Fig. 1. VLC has appeared as a com-

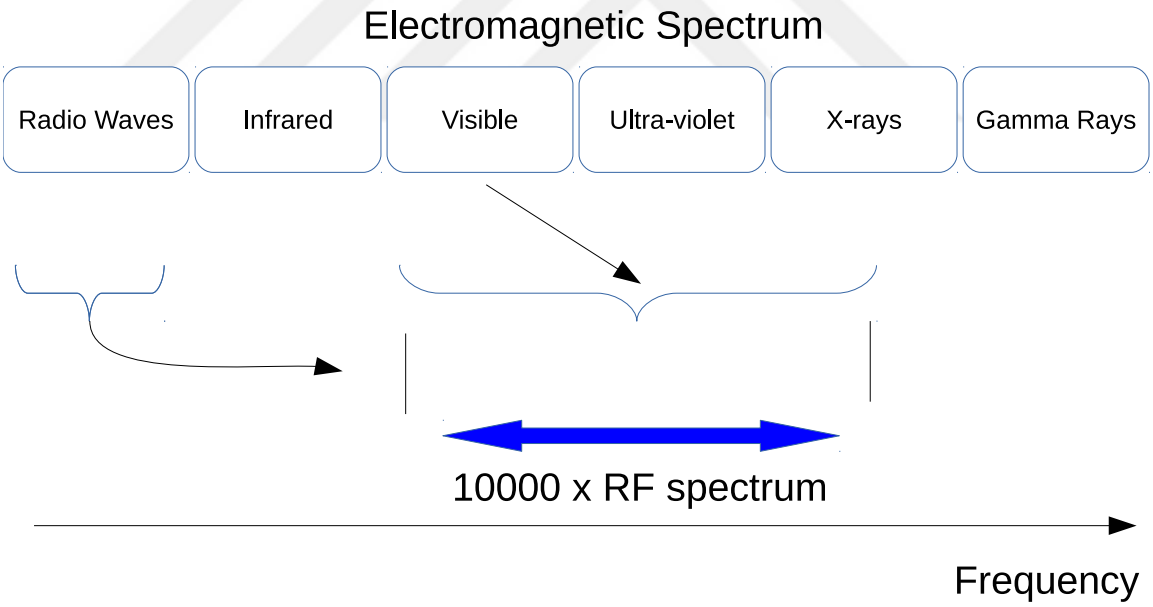

Figure 1. Electromagnetic spectrum and bandwith comparison between RF and visible light spectrums.

plementary technique to overcome limited RF spectrum. Significant properties of VLC involve unlicensed wide bandwidth, high security, energy efficiency and dual-use nature for both communication and illumination. Fifth generation (5G) wireless systems represent the next step of mobile telecommunications beyond the current

fourth generation (4G) standards. The next generation technology must be focused on higher system spectral efficiency, data rates, network capacity, scalability and reliability of communications, as well as lower battery consumption, cost, and so on. There are still arguments about the direction of future 5G technology. However, 5G technology should be significantly different from current communication technology standards with high performing physical layer system design. Traditional RF wireless communications have bottleneck to meet these demands such as occupied spectrum and energy efficiency etc. VLC serves both indoor and outdoor environment communications in future 5G systems.

2.2 VLC System Architecture

VLC architecture common layers are physical layer, MAC layer and application layer as shown in Fig. 2. Physical and MAC layers are defined in IEEE 802.15.7 standard.

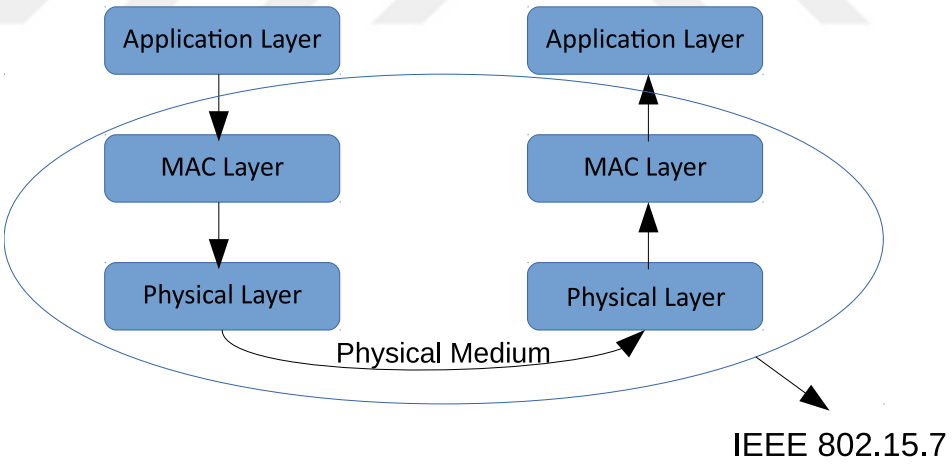

Figure 2. Layered VLC architecture comprising physical, MAC and application layers.

The physical layer comprises the physical specifications of the device and the relation between device and medium. The block diagram of typical physical layer of VLC architecture is shown in Fig. 3. The input bit stream is passed through the encoder. After encoding, modulation (such as ON and OFF keying, PPM and PWM etc.) is performed and finally, the data is sent through the LED for transmission

through the optical channel.

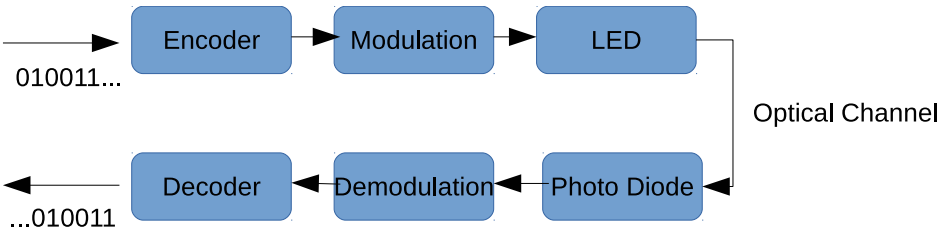

Figure 3. Fundamental physical layer block diagram of VLC [39].

Camera or imaging sensors are also utilized to receive the transmitted visible light signals from a display as shown in Fig. 4.

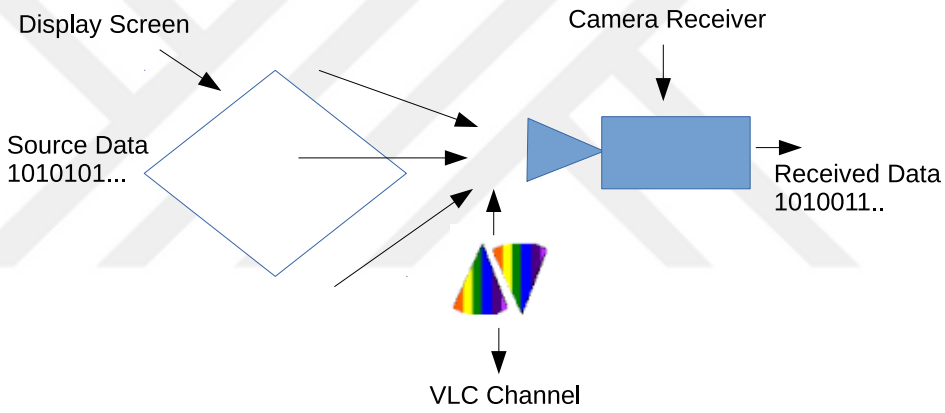

Figure 4. VLC architecture with display screen transmitter and camera receiver.

2.3 VLC Transmitter Architectures

In the transmitter side, we either utilize LED light bulbs or display screens as described in the following subsections.

2.3.1 LED Light Bulbs

The utilization of LEDs is increasing day by day with its high luminous efficiency, low cost, long lifetime and low energy consumption specifications. LEDs are utilized not only in indoor environments but also outdoors such as smart transportation systems as studied in [3]. Additionally, fast switching characteristics of LED makes it suitable

for VLC. The signal is easily modulated by On-Off keying method providing high data rates in comparison to traditional light sources such as incandescent light bulbs. In that way, communication and illumination are provided at the same time. Red-Green-Blue (RGB) LEDs or phosphor based LEDs function as VLC transmitters. RGB LEDs provide higher bandwith and data rates but it is more difficult in modulation.

2.3.2 Display Screens

LCDs are widely used in mobile devices, TVs and laptops. In VLC systems, display screens are also utilized as transmitter sources. Encoded information in display screens are decoded by a camera sensor. In [9], three main challenges such as perspective distortion, blurring and ambient light are discussed. In this thesis, we analyze and compare not only LCDs but also OLED type screens for VLC transmitter side.

2.4 VLC Receiver Architectures

In the receiver side, photodetector or camera based sructures are used as described in the following subsections.

2.4.1 Photodetector based Receivers

The photodetectors convert the received light into current. Modern commercial photodetectors easily sample the received visible light at rates of tens of MHz. As a long range outdoor study, in [7], 5.7 km range and tens of Kbps data rate are achieved with photodetector based receivers. In [9], they calculated the received optical power of a typical photodetector using spectral response of optical filter and multipath propagations with reflected paths. SNR calculations at the photodetector receiver based on shot and thermal noises are included. The ambient noise of solar radiation and artificial illumination sources such as lamps results in ambient noise floor which is a DC interference. The effect of such noise is mitigated by using a electrical high pass filter at the receiver.

2.4.2 Camera based Receivers

An imaging sensor or a camera sensor is utilized to receive the transmitted visible light signals. Since such camera sensors are available on most of mobile devices such as smartphones to capture videos and images, they have the potential to convert the mobile devices to VLC receivers. An imaging sensor consists of many photodetectors arranged in a matrix on an integrated circuit. However, the limitation of an imaging sensor is that the required number of photodetectors is very high in order to enable high resolution photography. This considerably reduces the number of frames per second (fps) that can be captured by the camera sensor. For example, frame rates of commonly used camera sensors in smartphones are smaller than forty. This means that direct use of camera sensor to receive VLC provides very low data rate [9]. Image sensor allows any mobile device with camera to receive VLC signal. However, in its current form, it only provides very limited throughput (few Kbps) due to its low sampling rate. Compared to a photodiode based receiver, a camera receiver provides more directional communication to achieve highly dense multiple-input and multiple-output (MIMO), since each pixel counts only as one element of the receiver.

CHAPTER III

OUTDOOR VISIBLE LIGHT COMMUNICATIONS

Outdoor VLC architectures concentrate on vehicular communications and traffic information systems in [2–5] with camera based receivers, and maritime communications in [6]. Outdoor enviromental effects such as wind speed and sea wave height are important design parameters for maritime communications. LED based lighthouse and beacons are utilized in maritime system as shown in Fig. 5. OOK modulation technique is utilized for the VLC transmission in [6].

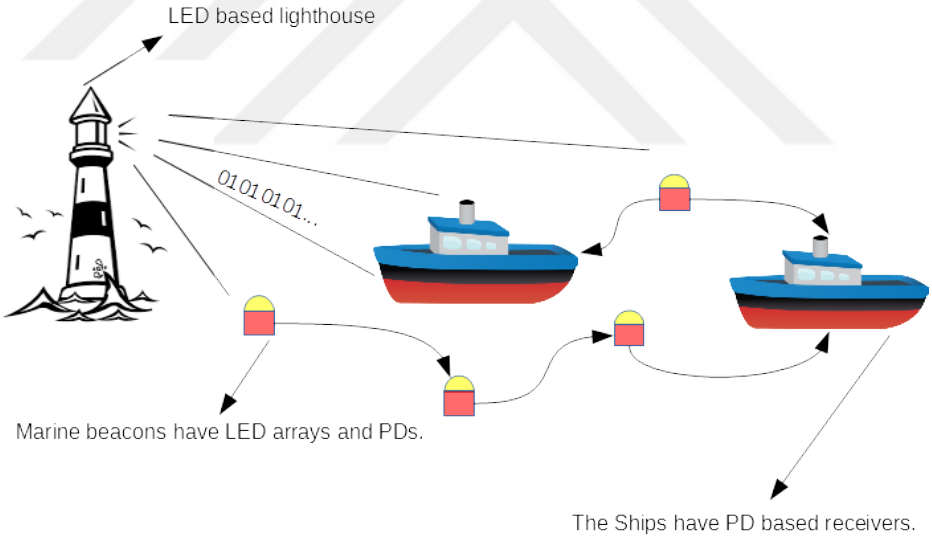

Figure 5. Maritime VLC channel model with LED based transmitters and PD based receivers [6].

The effect of higher focal length is discussed by emphasizing narrower field of view as a specific design issue [2,4,5]. In [2], an environmental adaptive transmission mechanism is proposed for vehicular applications. Dynamic traffic conditions and bad weather conditions are considered in [2] for long distance outdoor communications. Possible solutions including optical collection system and spectrum sensor array as

solutions for the problems of atmospheric attenuation and mitigating weather issues are also discussed. In [3], receiver diversity is utilized to achieve outdoor communications reaching hundreds of meters of range. Similarly, in other architectures, specific features of vehicular systems are emphasized while the ranges of communications are tens of meters except the maritime communications reaching several kilometers with very large transmitter and receiver detectors, and high power LEDs. In [7], 5.7 km range and tens of Kbps data rate are achieved with photodetector based receivers.

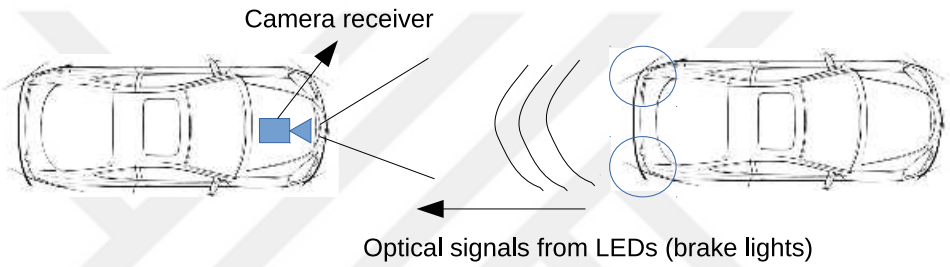

Figure 6. V2V outdoor VLC architecture with LED transmitter and camera based receiver.

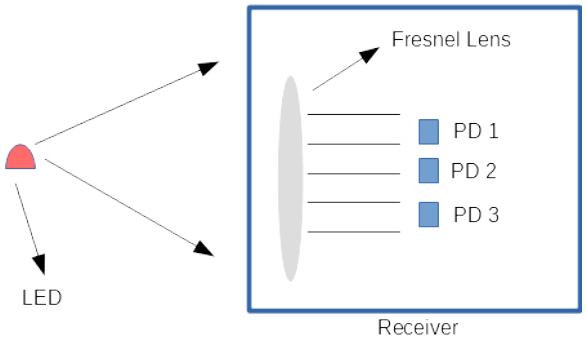

Figure 7. V2V communications with Fresnel lens based receivers.

The experimental analysis of VLC based V2V (Vehicle-to-Vehicle) communications under fog conditions is presented in [10]. A fresnel lens was used in receiver side for focusing the incoming light [10]. In that way, SNR performance of the system was increased under heavy fog conditions. Image sensors and photodiodes are used as receivers for LED based V2V communications. In Fig. 6, camera based receiver and LED transmitter communication model are shown.

TABLE II. Fundamental performance comparison of reference outdoor VLC architectures.

Reference	Receiver Type	Data Rate	Max Distance	Modulation Technique
[4]	Camera based	10-20 Mbps	2 m	OOK
[5]	Photodiode based	115 Kbps	31 m	OOK
[3]	Photodiode based	1 Gbps	100 m	QAM/OFDM
[7]	Camera based	9.6 Kbps	5.7 km	IM
[10]	Photodiode based	1 Kbps	1 m	OOK
[6]	Photodetector based	1 Mbps	2 km	OOK

Image sensor based method has an advantage in comparison with PD based method, since it offers a wider angle. However, image sensor based method obtains high cost, high power consumption and low processing speed, whereas PD based method has lower cost, lower power consumption and faster processing speed.

CHAPTER IV

NEXT GENERATION DISPLAY SCREEN VLC TRANSMITTERS

In this chapter, firstly, OLED, LCD and QD displays are described. Then, future display technologies are discussed. In addition, performance comparison of OLED, QD and LCD are performed in terms of response time, color gamut, spectral color output, contrast ratio and power consumption as summarized in Table III.

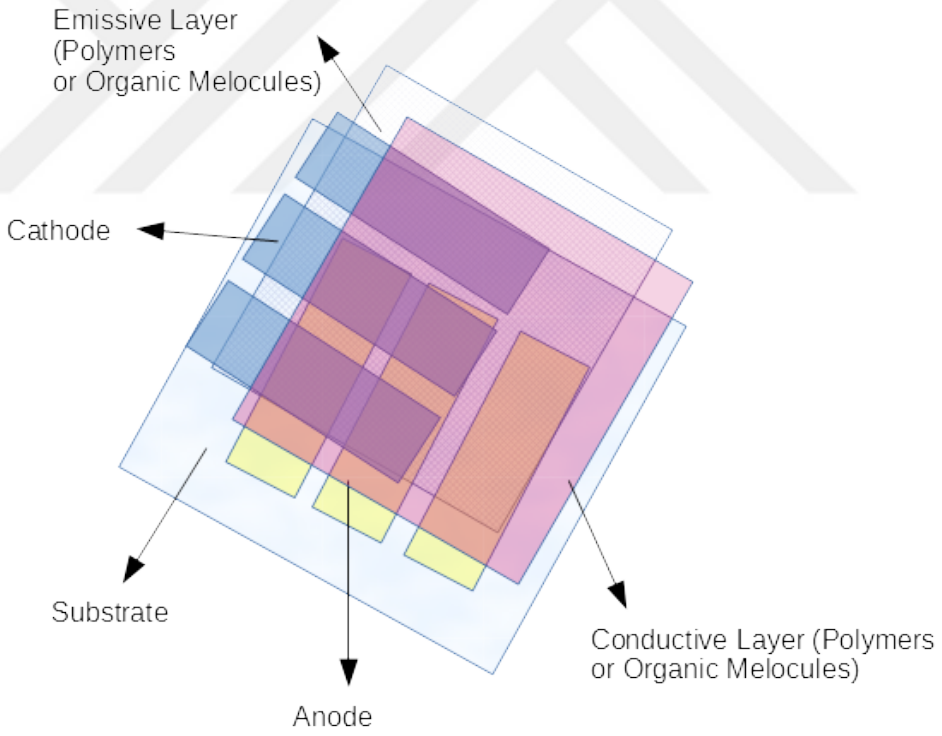

Figure 8. OLED sub-layers including substrate, anode, conducting layer, emissive layer and cathode.

4.1 OLED

OLEDs emit light when electricity is applied. They do not require a backlight. They have fast response times and infinite static contrasts.

Substrate, anode, conducting layer, emissive layer and cathode are sub-layers of a typical OLED as shown in Fig. 8. Conducting and emissive layers are made of organic plastic molecules. OLEDs do not require a backlight unit (BLU). Organic pixels of OLED display are self-emissive. OLED displays turn off each pixel completely which create perfect black and have approximately infinite contrast.

4.2 LCD

LCD has a sandwich structure consist of upper polarizer, bottom polarizer, glass substrates with thin film transistors, RGB color filters and liquid crystal as shown in Fig. 9. LCDs require a BLU in contrast to OLEDs.

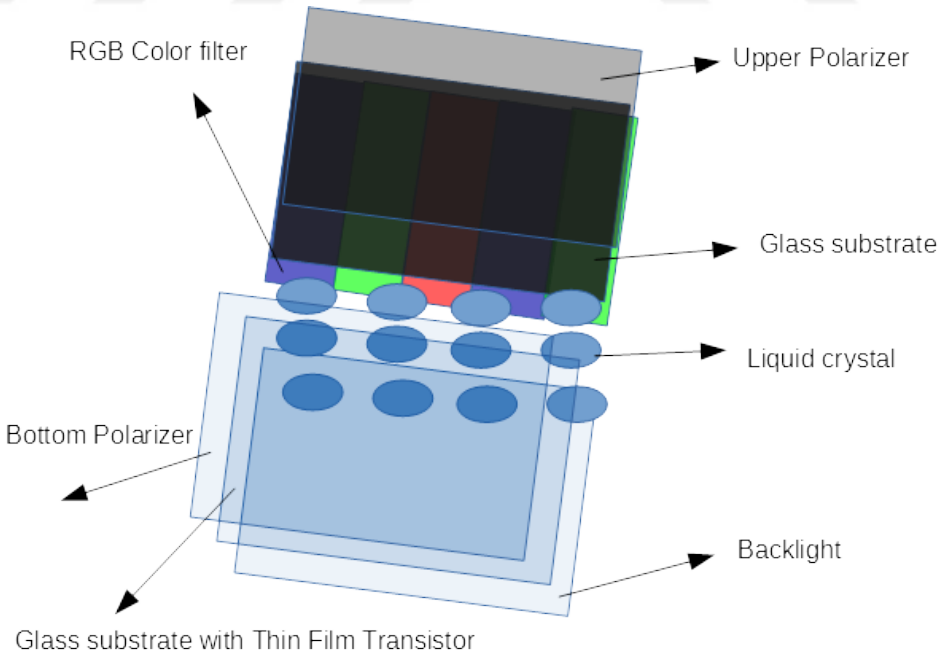

Figure 9. LCD sandwich structure consists of upper polarizer, bottom polarizer, glass substrates with thin film transistors, RGB color filters and liquid crystal.

4.3 QD

The differences between QD and LCD display screens are the utilization of quantum dot enhancement film (QDEF) instead of diffuser film and blue LED instead of yellow phosphor covered LED as shown in Fig. 10 [11,12]. The QDEF contains red and green emitting quantum dots. QDEF based displays have higher color gamut in comparison with LCDs.

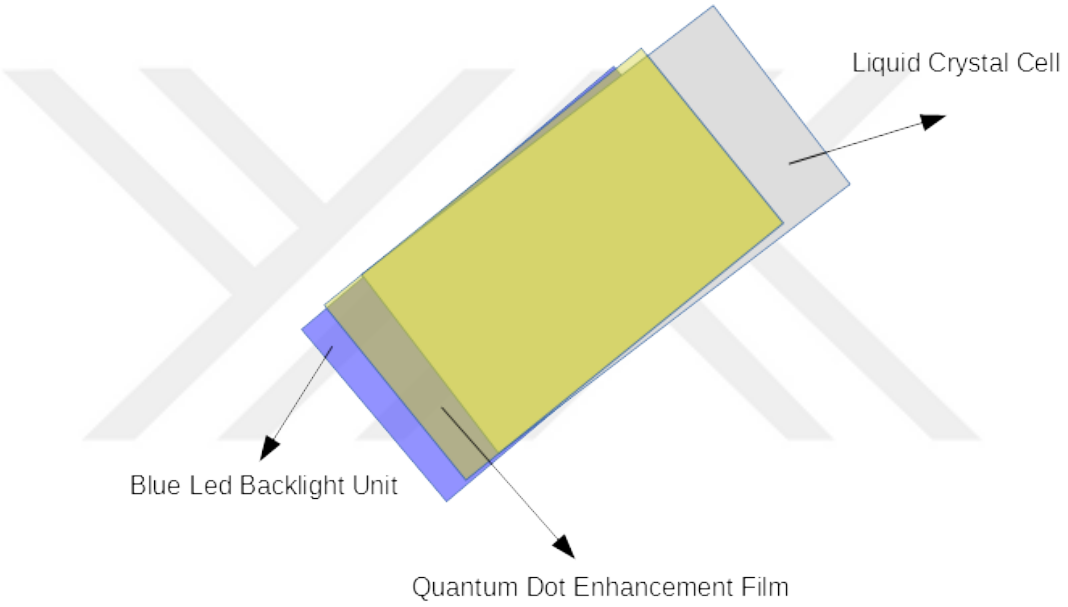

Figure 10. QD display structure (Blue LED + QDEF).

4.4 Future Technologies

Bendable displays, foldable smartphones, holographic displays, transparent displays are some of the future technologies for next generation display technologies. These systems improve flexibility, power efficiency and VLC communication performance parameters such as range, coverage and viewing angle.

4.5 Comparison between Screens

Display technologies are compared in terms of response time, power consumption, lifetime, spectral performance, CG and static contrast by emphasizing their effects

on VLC performance as summarized in Table III. Next, each performance parameter compared in Table III is discussed in more detail.

TABLE III. Comparison of display technologies for VLC performance.

	QD	OLED	LCD	**Effect on VLC**
Response Time (ms) [13, 14]	< 1	< 0.01	< 1	**Rate**
Static Contrast [14, 47]	5000:1	Infinite	5000:1	**Constellation and Power**
Lifetime (hours) [12, 16, 17]	20K - 30K	30K - 50K	30K - 60K	**Total Data**
Color Gamut [11, 18–20]	$> 100\%$	$> 100\%$	$\approx 70\%$	**Min. symbol distance**
Spectrum perform. [11, 12, 19]	High	High	Low	**Less Interference**
Power Efficiency [11, 15]	110%-150%	60%-110%	100%	**Power**

4.5.1 Response Time

The response time of OLEDs is ≈ 0.01 ms which is several hundred times faster than sub-millisecond response times of LCD and QD displays utilizing in-plane switching blue phase LCD technology [13, 14]. Therefore, OLED provides higher VLC data transmission rates along with elimination of blur effect. The differences between QD and LCD display screens are the utilization of QDEF instead of diffuser film and blue LED instead of yellow phosphor covered LED [11, 12]. Therefore, LED and QD displays have similar response times depending on liquid crystal.

4.5.2 Power Consumption

The energy consumption of the screen to achieve a desired level of brightness directly effects VLC performance. The efficiencies are compared by directly considering the radiated light intensity and by excluding the consumption in the remaining components of TVs. The average luminous efficiency of OLEDs reaches 60 lm/W while LEDs reach 100 lm/W efficiencies [15]. However, OLED TVs are more efficient in

terms of the absence of back light unit (BLU) providing an improvement of 10% compared with LCD. Therefore, OLED TVs have varying levels of energy efficiency, i.e., their efficiencies are between sixty percent less and ten percent more compared with LCD display screens in order to simulate performance variations in different OLED related consumer products. Besides, QD displays are ten to fifty percent more power efficient compared with LCDs due to more transmissive color filters and less amount of light to provide the desired display brightness [11].

4.5.3 Overall Lifetime

The lifetime of display screens determines the overall amount of VLC based data transmission. The limited lifetime of OLEDs due to blue OLEDs with $\approx$ 14000 hours of lifetime has been improved with advanced materials exceeding 50000 hours of lifetime in the products currently in the market [16, 17]. Additionally, LED lifetime is between 30000 and 60000 hours while the lifetime of QDEFs is between 20000 and 30000 hours before the luminance drops by 15% [12, 16]. So, OLED is a good candidate as a long lasting and high performance VLC transmitter.

4.5.4 Spectral Performance

QD displays radiate light with narrow spectral distribution with the peak wavelength based on the size of the quantum dot. Separate narrow emission spectrum of QDs provides minor interference between RGB components as shown in Fig. 11 [11]. QDs have full width at half maximum (FWHM) values of between 30 and 40 nm for the spectral components [11, 12]. This results in a higher CG and less interference between different CSK modulated VLC symbols. However, white LEDs with (yttrium, aluminum, garnet) (YAG) phosphor include concentrations of non-primary intermediate colors leaking through the color filter and less saturated red and green spectral components as shown in Fig. 11. Besides, OLED and QD displays have similar performances for high performance CSK modulation based on the experiments with

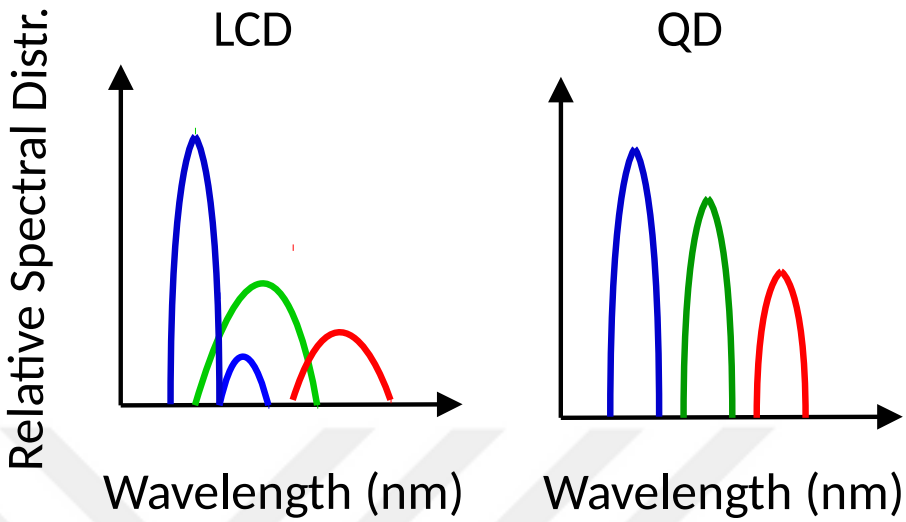

Figure 11. Spectral output of LCD and QD display screens [11] while OLED displays have similar performance with QD as experimented in [19].

active matrix OLED (AMOLED) displays in [19].

4.5.5 Color Gamut

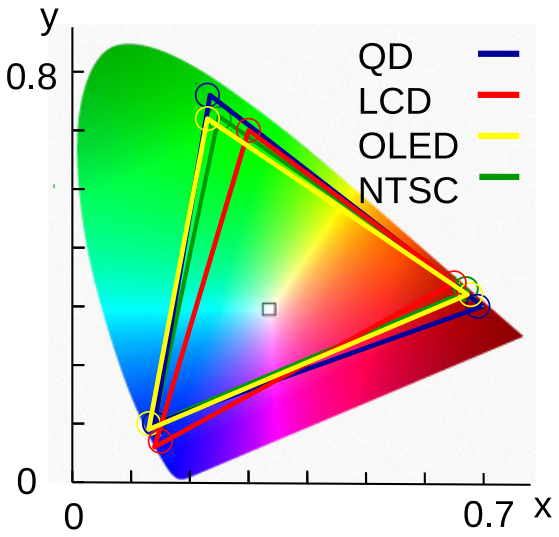

Figure 12. Color gamut comparison of QD, LCD, OLED and NTSC in CIE 1931 color space chromaticity diagram [11, 18–20].

A color gamut simply is explained as range of colors allowed for a video signal. QD and OLED displays have larger CG area exceeding National Television System

Committee (NTSC) standard [18, 19]. Additionally, LCD displays have lower CG compared with NTSC [11, 20]. Higher CG improves the minimum symbol distance for CSK modulated VLC channels. CGs of OLED, QD and LCD displays compared with NTSC are shown in Fig. 12 while chromaticity values are provided in Table IV.

TABLE IV. Reference color gamut values of display technologies.

	NTSC		QD [18]		OLED [19]		LCD [11, 20]	
	x	y	x	y	x	y	x	y
R	0.670	0.330	0.700	0.280	0.680	0.300	0.640	0.339
G	0.210	0.710	0.200	0.760	0.200	0.720	0.286	0.596
B	0.140	0.080	0.140	0.080	0.130	0.080	0.145	0.057
CG	100%		117%		106%		72%	

4.5.6 Static Contrast

QD displays and LCDs have similar contrast levels reaching static ratios of 5000:1 [14,47]. On the other hand, OLED displays have perfect black level which is obtained by turning off the pixels completely. Ultra-high contrast ratio supports higher order constellation for VLC and reduces energy consumption for the set of symbols with low brightness. Therefore, OLED has significant energy efficiency compared with QD and LCD display screens.

CHAPTER V

LOW COST WIRELESS INTERNET SERVICE PROVIDING ARCHITECTURES

There are low cost wireless ISP architectures for rural and suburban areas as alternative systems compared with the proposed hybrid VLC and RF system. It is very crucial since more than half of the world population has still no internet access.

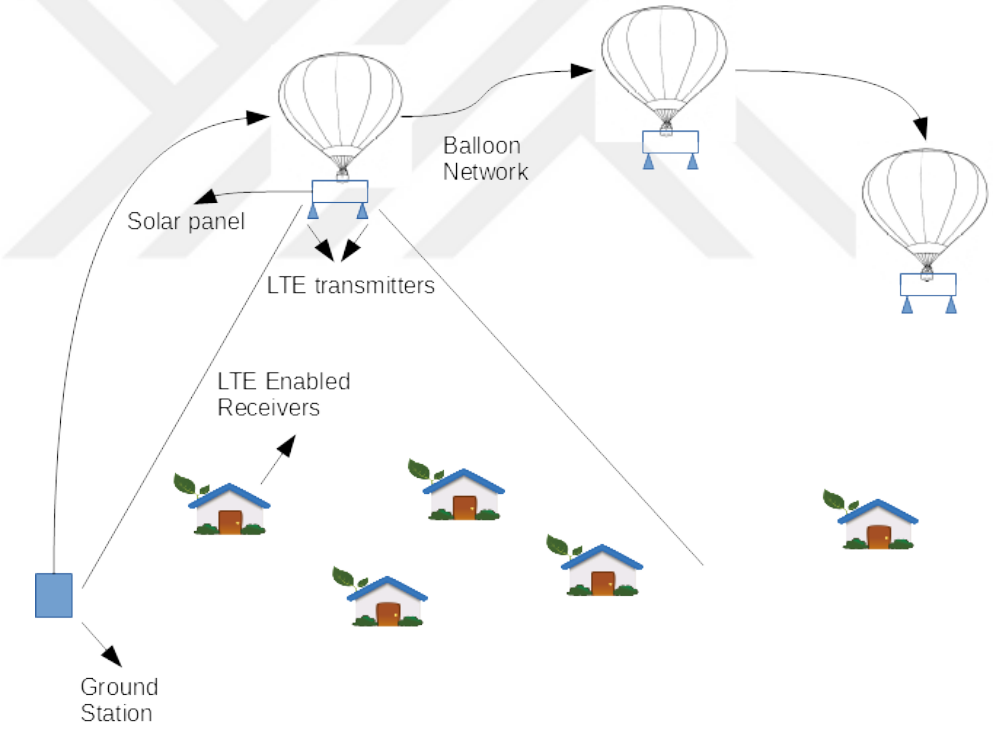

Figure 13. Wide area network with multiples of balloons by X company, Project Loon [21].

Firstly, the project denoted by Loon by X company (formerly Google X) is discussed. Project Loon aims to launch a fleet of balloons to provide internet coverage to users on the ground by carrying LTE signals. Wide area network with multiples of balloons is created. The system launches a new balloon every 30 minutes. The

TABLE V. X company Project Loon vs Facebook Aquilla comparison based on power source, coverage and operating areas.

	Project Loon	Facebook Aquilla
Power Source	Solar	Solar
Coverage Area	5000 km^2	7310 km^2
Operating Area	Stratosphere (20 km up)	Stratosphere(18-27 km)

Project Loon balloons survives the conditions in the stratosphere. Ground station sends signals across balloons, and back down to users' LTE enabled phones. The equipment is solar powered for lowering energy costs [21].

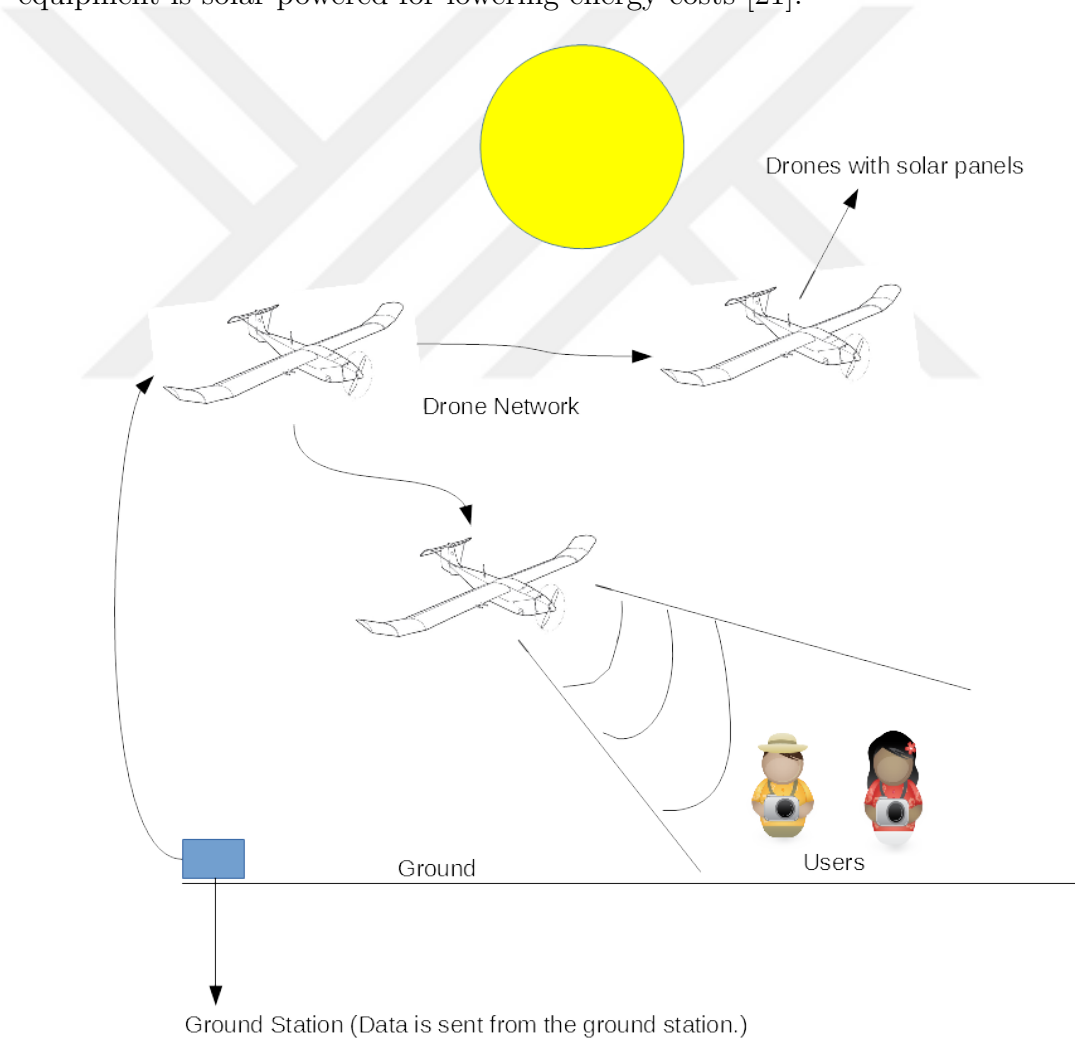

Figure 14. Internet by drone project denoted by Facebook, Project Aquilla [22].

Facebook has the same target with X company. In this system, drones try to create a network in the sky for rural areas. The drones are solar powered. The drone

network is created by connecting to each other with lasers [22].

Data is sent from the ground to one aircraft via RF or laser. Then, signals are transmitted to other drones via laser as shown in Fig. 14. As a result, drones provide internet access to users on the ground via RF.

These projects are promising since drones or balloons cost much less than satellites. In Table V, these two projects are compared based on their power source, coverage and operating areas.

CHAPTER VI

HYBRID VISIBLE LIGHT COMMUNICATION TECHNOLOGIES LITERATURE REVIEW

VLC is combined with existing OWC technologies such as RF and IR in various hybrid architectures. In addition, VLC system structures using power line communication (PLC) also exists for achieving fast and economic indoor communication. In the next sections, hybrid VLC systems in the literature are examined.

6.1 VLC-RF Hybrid System

RF and VLC indoor hybrid scheme proposed in [23] utilizes both WiFi and VLC. VLC channels are adopted to support RF communications for dynamically distributing resources. A handover mechanism between WiFi and VLC improves system throughput. In this way, it provides bandwith advantage of VLC architecture and integration with RF devices. The system includes VLC hotspots and a WiFi Access Point (AP) as shown in Fig. 15.

In [24], router and WiFi AP are connected to LEDs to provide hybrid RF-VLC communication. Mobility of users and the field of view of photodetectors are also considered in the design. Mobile terminal (MT) connects to the WiFi AP when it is out of coverage area of LEDs. MTs are in relay mode for other MTs not in the coverage area. In [8], a hybrid VLC and RF femtocell system is proposed while exploring user connection issues to achieve effective load balancing.

6.2 VLC-PLC Hybrid System

In contrast to existing hybrid VLC and RF systems, PLC and VLC scenario suggests the use of PLC to coordinate and provide data to the VLC transmitters in [26]. Block

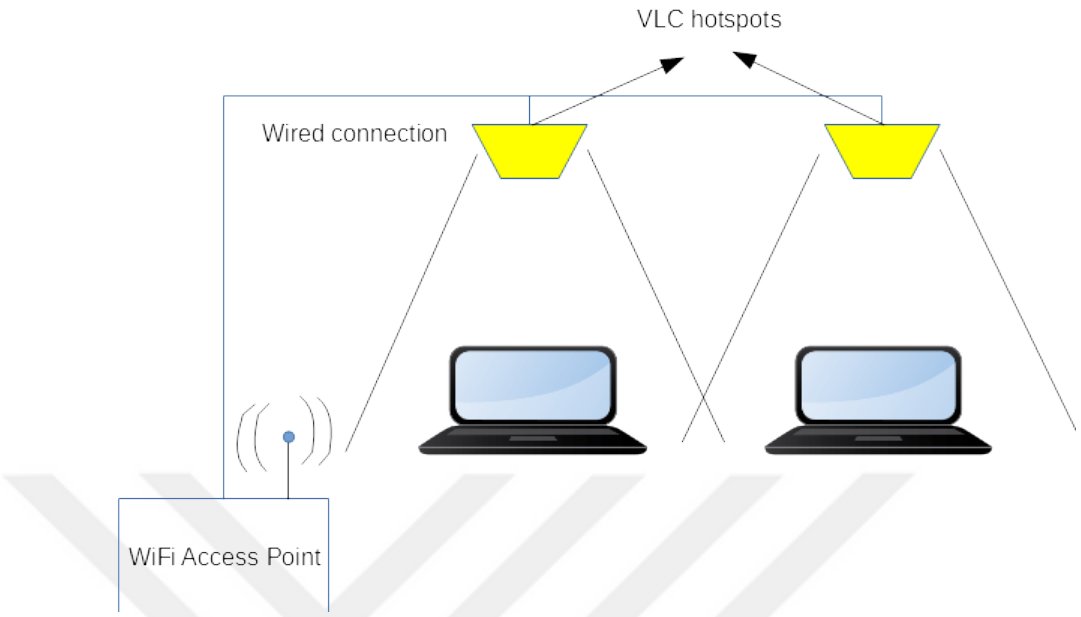

Figure 15. WiFi-VLC hybrid system with VLC hotspots and WiFi AP [23].

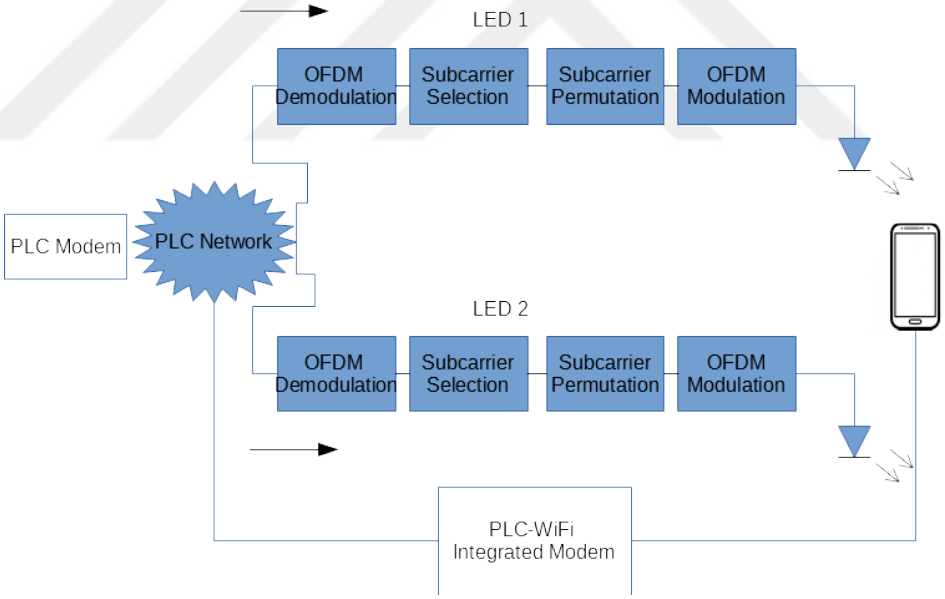

Figure 16. VLC-PLC hybrid system block diagram combined with PLC modem and LED transmitters [26].

diagram of VLC-PLC system is shown in Fig. 16. The LED light source is placed on the ceiling for easy implementation. The power line sends data and coordinate the communication through multiple LEDs. Then LEDs forward the received PLC data to users.

In [27], hybrid VLC system using existing PLC infrastructure is proposed to achieve a basic system design. In this integrated structure, a VLC system is connected directly to the existing power line. It emits the baseband signals of power line by LED elements in the room. Simulations show the feasibility of the suggested system in terms of the illumination and SNR performance [27]. The demonstration presents a data rate up to 100 Kbps.

6.3 VLC-IR Hybrid System

VLC systems provide dual combination of lighting and communications. The uplink channel design is challenging because of mainly energy limitations. In [28], the uplink challenge in indoor VLC is solved by the use of an infrared (IR) link. A fast adaptive beam steering IR system (FABS-IR) is proposed to increase the uplink performance at high data rates. The goal of the system is to enhance the received optical power signal and reduce the channel delay spread when the system operates at a high transmission rate.

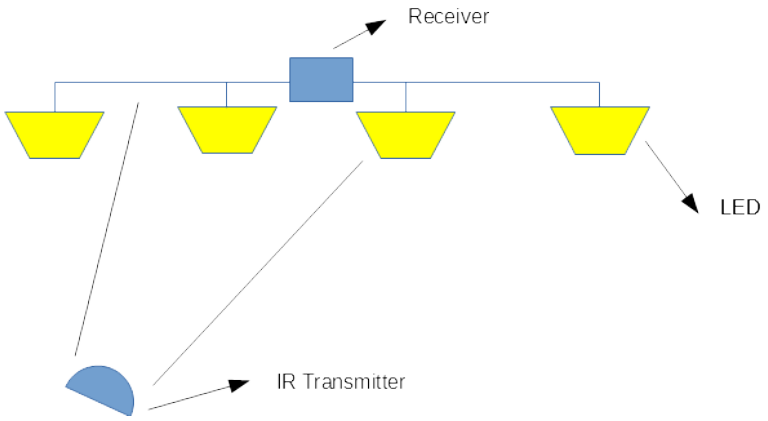

Figure 17. IR uplink system for hybrid VLC-IR architecture [28].

In [29], a hybrid diffuse infrared transmitter (HDIrT) combined with an imaging receiver is proposed to support VLC system when the light is dimmed or is totally turned off. IR optical communications boasts similar advantages as VLC systems. It provides high transmission rates. The ultimate aim of this system is to increase the

signal to noise ratio (SNR) and to mitigate the channel delay spread when the system operates at a high data transmission rate.

CHAPTER VII

PROPOSED HYBRID VLC-RF ISP INFRASTRUCTURE

In this chapter, uplink and downlink of the hybrid VLC-RF ISP system is described in detail. Furthermore, IM based capacity channel for display screen based transmitters and probability bit error formulas are clarified.

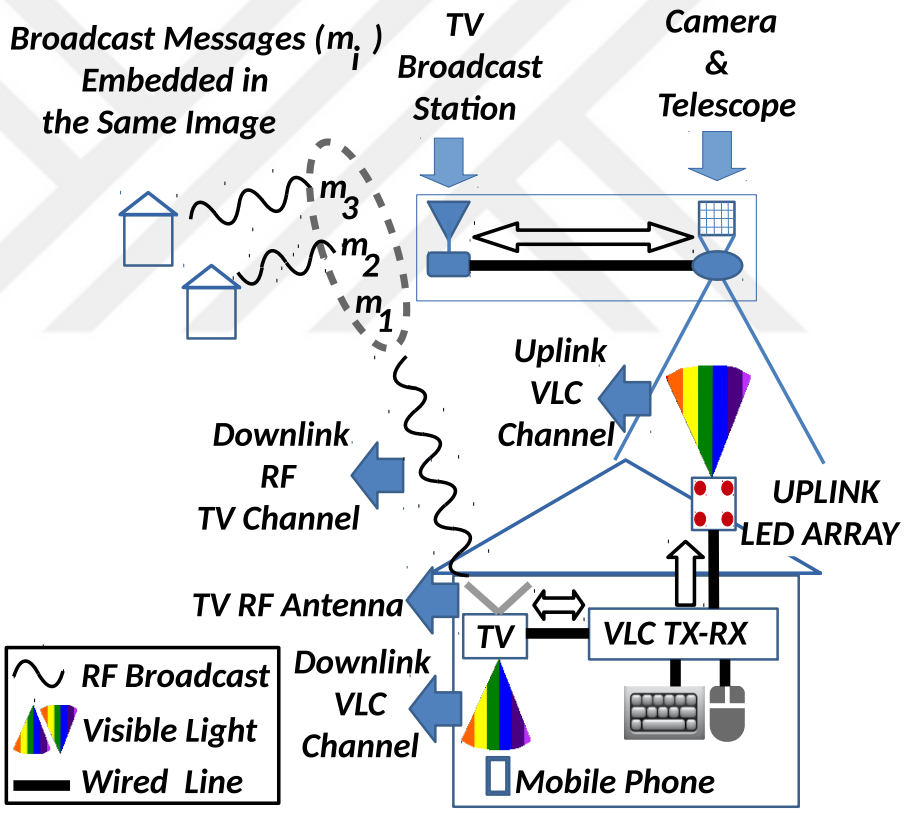

Figure 18. VLC uplink and hybrid downlink system architecture combined with TV RF broadcast.

7.1 System Model for Uplink

The uplink channel is achieved by utilizing low cost CCD cameras and telescopes with the novel architecture in Figs. 18 and 19. The receiver array is composed of single

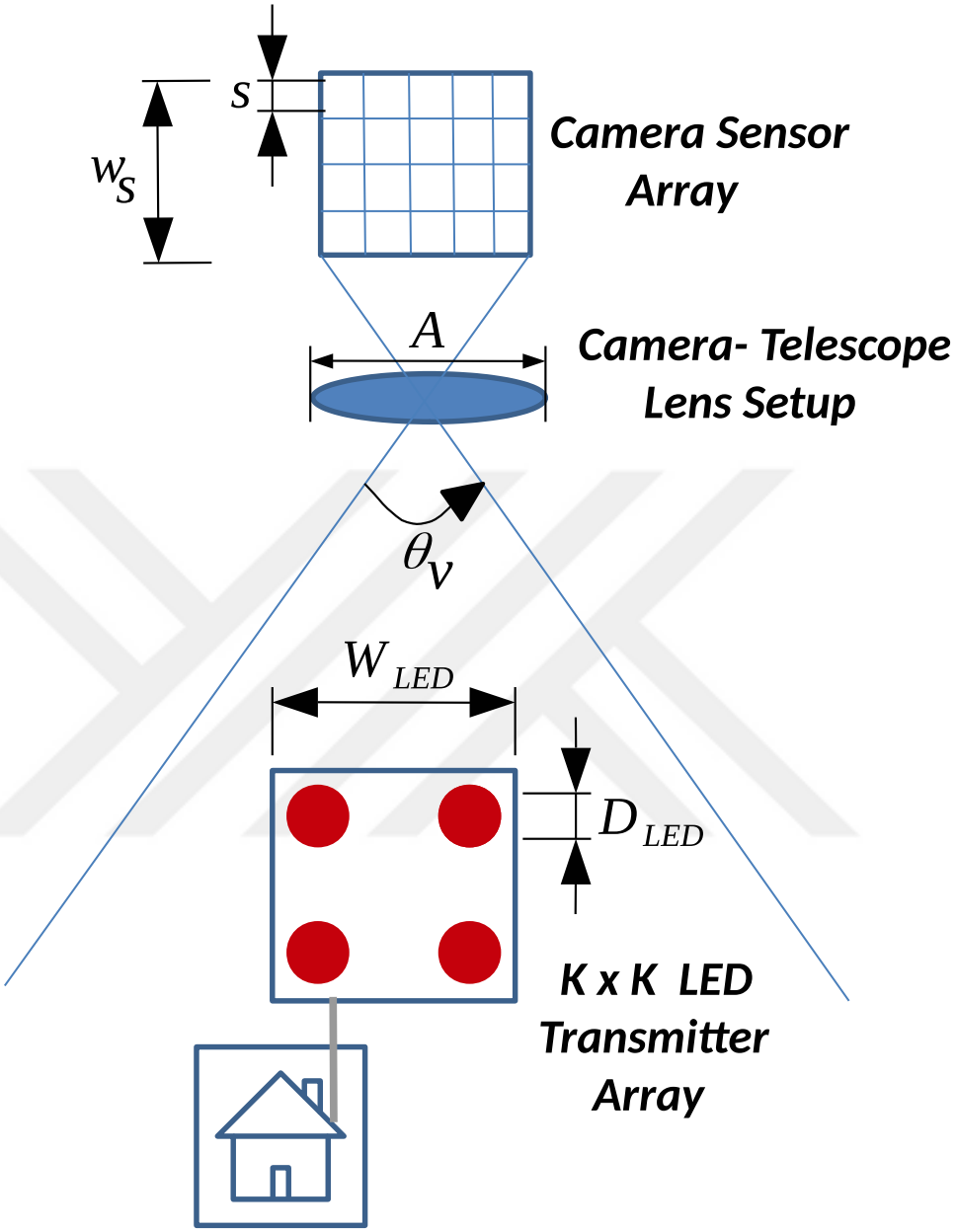

Figure 19. Detailed uplink channel model between a camera receiver supported by a telescope and a LED array.

units including a telescope and a camera in Fig. 19 such that each telescope observes a specific set of LED array transmitters located near a specific region. A multiple of telescopes with long focal lengths f_{eff} is utilized to cover the whole area similar to a cellular VLC concept as shown in Fig. 20. In modeling the basic architecture, a 2D model is assumed to discover the main formulation and simplification. The angle of

view is defined with respect to the effective focal length f_{eff} as follows:

$$\Theta_v = 2 \arctan \frac{w_s}{2\, f_{eff}} \tag{1}$$

where w_s is the horizontal or vertical dimensions of camera sensor. Then, for a coverage area of 360°, the number of telescope camera receivers needed for communication with LED panels at a distance d is given by $N_T = 360° \,/\, \Theta_v$ with Θ_v defined in terms of degrees. The resolution with respect to specific focal length and distance is given by the following [30]:

$$\Delta_{LED} = \frac{d\, 1.22\, \lambda}{A \cos(\varphi)};\ \Delta_s = \frac{f_{eff}\, 1.22\, \lambda}{A \cos(\varphi)} \tag{2}$$

where Δ_{LED} and Δ_s are the minimum distances between perimeters of LEDs in real and image planes, respectively, d is the distance between the LED array and the camera, φ is the angle between the camera image plane and LED array, A is the diameter of the aperture and λ is the wavelength. For simplicity, we assume the planes of LEDs and the camera are parallel and we consider a 2D architecture, e.g., the panels and the telescope have equivalent height. We assume that each LED panel on the roof of a house is formed of $K \times K$ LEDs with diameter D_{LED} separated by Δ_{LED} resulting a total length or width of the panel equal to $W_{LED} = K\,(D_{LED} + \Delta_{LED}) + \Delta_{LED}$. The LED arrays are assumed to be distributed with the distance d_h between houses. Then, the following is obtained to determine the number of served houses, i.e., N_h, in a single telescope cell for given d, d_h, w_s and f_{eff}:

$$N_h \;\; = \;\; d\, w_s \,/\, (f_{eff}\, d_h) - 1 \tag{3}$$

and the number of pixels where each LED covers is as follows:

$$\mathrm{Px}_{LED} = \frac{f_{eff}\, D_{LED}}{d\, s} \tag{4}$$

where s is the physical size of the pixel.

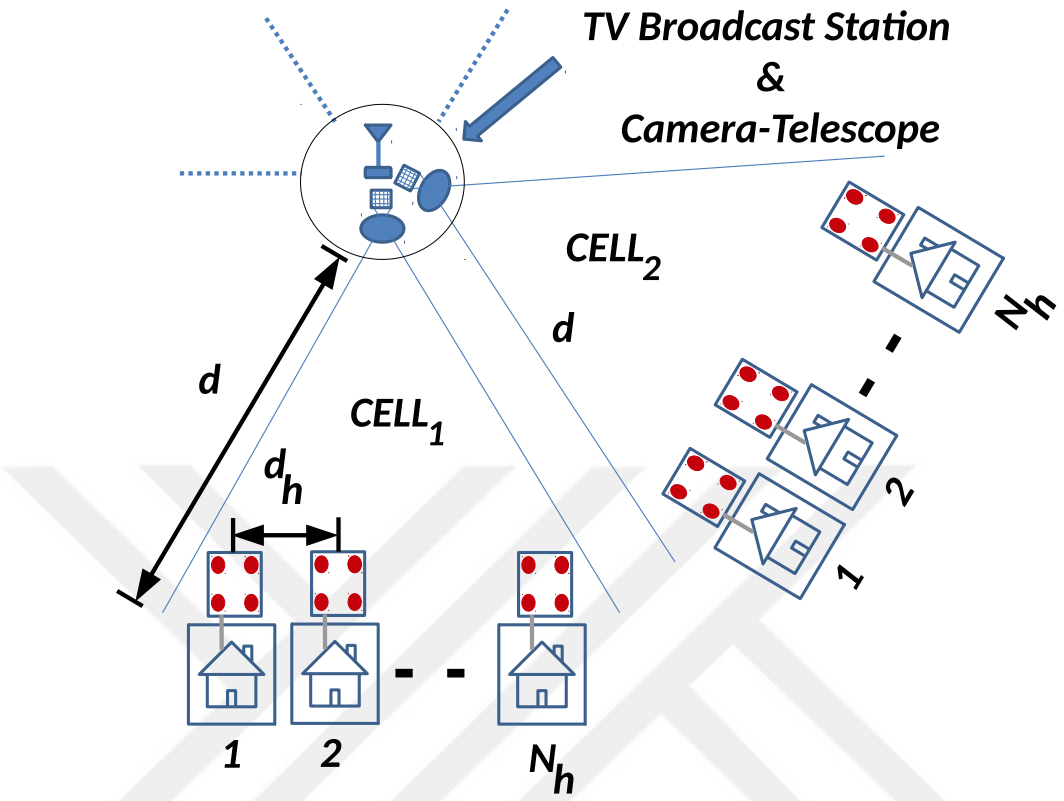

Figure 20. Cellular, outdoor and long range VLC with multiple telescopes.

The channel between LED panels on top of the houses and the telescope camera experiences various detrimental effects of outdoor environment, e.g., fog, rain, snow, wind and other weather conditions which can reduce the received power or change the position of the LED panels. The most severe for VLC among these is the fog. The empirical model including the effects of fog in terms of attenuation is modeled for VLC in [10,31] as $\gamma_\lambda = (17.35\,/\,V)(\lambda\,/\,550)^{-\alpha}$ where γ_λ is the attenuation coefficient (dB/km), V is the visibility range in kms, λ is the wavelength in nm and the parameter α is a function of the visibility range V for various air conditions from clear sky to heavy fog. Morever, it is assumed that the effect of sun light ambient noise is reduced by specific placement and design of the receiver units [31,32]. Moreover, scintillation is neglected for ranges of several kms communications. Then, the received current at a pixel with index (i, j) on camera sensor array due to a LED at a view angle of $\Theta =$

$\psi < \Theta_v$ as demonstrated in Fig. 19 is given by the following [31, 43]:

$$I_R^{\Theta}(i,j) = \quad P_T^{\Theta}\, 10^{-\gamma_\lambda\, d\,/\,10^4}\, g(\psi)\, T_s(\psi) \cos(\psi) \\ \times \frac{A_{ij}\, R_p\, D_{LED}^2 \cos^m(\Theta)\,(m+1)}{8\, d^2} \tag{5}$$

where $A_{ij} = 4\, s^2 \,/\, \big(\pi(\mathrm{Px}_{LED}\, s + \sigma_b)^2\big)$ is the proportional area of the pixel compared with the total image area of LED as defined in [33], σ_b is the lens Gaussian blur standard deviation defined as the ratio of minimum distance between image circumferences on the image plane to $2\sqrt{2\ln 2}$ in [33] or $\Delta_s \,/\, (2\sqrt{2\ln 2})$ in our model, R_p is the responsivity of a sensor pixel in (A/W), $m = -\ln 2 \,/\, \ln(\cos\Phi_{1/2})$, $T_s(\psi)$ is the signal transmission coefficient of an optical filter, $g(\psi) = n^2 \,/\, \sin^2(\Theta_v)$, n is the internal refractive index of the optical concentrator and $\Phi_{1/2}$ is the transmitter semi-angle at half power. If it is assumed that the focal length and the number of telescope cameras are chosen in a way to discriminate all the single LED units then, the capacity for a single color LED at the angle Θ in an intensity modulation framework is given as follows for camera sensor devices [33]:

$$C_{LED,\Theta} \approx K^2\, W_r\, \log_2\left(1 + \frac{\sum_{i,j\in S_\Theta}\big(I_R^{\Theta}(i,j)\big)^2}{\sum_{i,j\in S_\Theta}\big(\sigma_n(i,j)\big)^2}\right) \tag{6}$$

where $\sigma_n(i,j) = \sqrt{2\, q\, R_p\, P_n\, s^2\, W_r}$ is the noise current at the pixel (i,j), P_n is the shot noise power per unit area, q is the electron charge, W_r is the frame rate of the camera and S_Θ includes the index of the pixels covered in the image area of the LED on the camera, i.e., $\big(\pi(\mathrm{Px}_{LED}\, s + \sigma_b)^2\big) \,/\, 4$.

Indoor uplink unit is connected with TV (as a monitor) through a low cost device including VLC transmitter circuit (Tx) modulating uplink data and driving LEDs on the panel, VLC decoder circuit (Rx) extracting the data embedded in TV image due to downlink RF broadcast and input devices, e.g., a keyboard and a mouse, as shown in Fig. 18. The device is realized by combining low cost hardware, e.g., Raspberry Pi, as a personal computer and LED driving circuit.

7.2 System Model for Downlink

The downlink channel is formed in a hybrid mechanism as shown in Fig. 18 synchronizing TV RF broadcast of multimedia data and the transmission of the information embedded in the multimedia to either mobile phone through VLC *wireless* channel or low cost VLC Rx device through *wired* connection with the TV. Since data is transmitted from broadcast station in the form of images with a VLC encoding approach, it is not necessary to use extra hardwares in the station or TV other than the generation of encoded data in the station and decoding the data in VLC RX device. It is important to realize a multi-user encoding architecture storing data in the form of images containing downlink data of multiple users which is best suited to TV RF broadcast channels. In addition, TV broadcast station should be synchronized with uplink camera receivers connected with high speed wired line in order to achieve two-way communication. Data link and MAC layer protocols achieving the hybrid communication should be designed. The bottleneck of the downlink hybrid communication architecture capacity is the maximum amount of intensity or color coded multimedia data capacity which includes all of the information symbols of the served houses in a combined manner. This reaches hundreds of Mbps multimedia data with tens of broadcast channels while each of them having capacity of tens of Mbps and 8 MHz in UHF bands [34]. This data rate is enough to provide downlink capacity of several Mbps to hundreds of houses at the same time. Each house extracts the requested information from the same multimedia image displayed on the screen with some predetermined protocol between the TV broadcast station and the uplink transmitter of a specific house. A cross-layer approach is necessary synchronizing downlink and uplink channels including hybrid RF, indoor and outdoor VLC channels. Therefore, there is a set of challenges to be solved to realize the prototype system design as summarized in Section 10.

VLC indoor wireless architectures based on display transmitters and camera receivers are considered in this work [35, 36]. Information is modulated through either intensity modulation (IM) or color shift keying (CSK). Spatial diversity creates a MIMO channel model [35]. It is observed that hundreds of Mbps data rates are achieved by utilizing high definition (HD) screens and 100 Hz frame rates [37]. Two different capacity performance metrics are compared for different display technologies, i.e., IM based capacity denoted by C_I for MIMO display screen to receiver camera communication channel and probability of bit error performance denoted by P_e^b for color shift keying (CSK) based modulation.

7.3 Intensity Modulation

IM based channel capacity expression in [35, 36] is modified by including intensity factor k_I^x as the following:

$$C_I = W_r \, W_{px} \, \log_2 \left(1 \, + \, k_I^x P_T \, h_d \, / \, \sigma_n^2\right) \tag{7}$$

where C_I (bit/s) is the capacity, W_r is the frame per second, W_{px} is the resolution of each frame, P_T is the average transmit power of each symbol, h_d is the channel response at the receiver distance d, $P_R = P_T \, h_d$ is the average received power, σ_n^2 is the average noise energy and $k_I^x P_R \, / \, \sigma_n^2$ is the SNR at each receiver pixel. k_I^x is a factor without unit which models the energy efficiency of each display screen denoted by x, i.e., LCD, OLED or QD, in terms of radiated optical intensity or power with respect to the transmitter power feeding the display. In Section 8.2, k_I^{LCD} is chosen to be equal to one as a reference value. It is assumed that the receiver camera array is formed of high speed photodetectors capable to receive at the frame refreshing rate of the display. Furthermore, each transmitter pixel is associated with a single pixel in a perfectly compatible and focused camera receiver for calculating the boundary performance and the resulting channel is denoted by pixel-to-pixel (Px2Px) communication channel.

7.4 Color Shift Keying Modulation

Display screens are capable of producing CSK modulated VLC by changing the colors of the individual pixels. If all the symbols are assumed to be transmitted with equal probability for M-CSK where M is the order of the constellation then, the union bound of the probability of symbol error per channel use for each independent Px2Px channel is given by $P_e^s \leq (0.5\,/\,M)\sum_{m=1}^{M}\sum_{k=1,k\neq m}^{M} P(\widehat{k}|m)$ where $P(\widehat{k}|m)$ is the probability that $d_{\mathbf{s_k},\mathbf{r}} < d_{\mathbf{s_m},\mathbf{r}}$ and $d_{\mathbf{s_k},\mathbf{r}}$ is the distance between the CSK symbol $\mathbf{s_k}$ and the received chromaticity value denoted by $\mathbf{r}$ [44, 45]. The demodulation is achieved in xyY color space domain to better emphasize the effect of CG on the minimum distance between symbols with fixed receiver CSK symbol power [45, 46]. The central chromaticity values of red, green and blue (RGB) color basis are marked with circles in International Commission on Illumination (CIE) 1931 color space chromaticity diagram as shown in Fig. 12 where (x_k, y_k) for $k \in [1, 3]$ corresponds to central wavelengths of three LEDs. The set of RGB chromaticities for the samples taken from the literature for different display screen technologies is summarized in Table IV where NTSC is chosen as the reference gamut. OLED and QD screens have larger color space compared with LCD. The intensity corresponding to kth LED for mth CSK symbol denoted by P_{mk} satisfies $[x_r\ y_r]^T = [\mathbf{x}\ \mathbf{y}]^T(\mathbf{P_m} + \mathbf{n})$ where (x_r, y_r) is the received chromaticity value, $\mathbf{x}^T \equiv [x_1\ x_2\ x_3]^T$, $\mathbf{y}^T \equiv [y_1\ y_2\ y_3]^T$, $\mathbf{P_m}^T \equiv [P_{m1}\ P_{m2}\ P_{m3}]^T$, $\sum_{k=1}^{3} P_{mk} = 1$ W and $\mathbf{n}^T \equiv [n_1\ n_2\ n_3]^T$ is the additive white Gaussian noise (AWGN) vector. Each n_k for $k \in [1, 3]$ is independent and identically distributed with power spectral density of $N_0\,/\,2$ at the receiver for the corresponding wavelength of kth LED. If we assume that mth symbol is transmitted then, $d_{\mathbf{s_k},\mathbf{r}}$ is defined as $d_{\mathbf{s_k},\mathbf{r}} = |\,[\mathbf{x}\ \mathbf{y}]^T(\mathbf{P_m} + \mathbf{n}) - \mathbf{s_k}|$. Then, $P(\widehat{k}|m)$ is easily obtained by explicitly calculating the probability of $P\big(|\,[\mathbf{x}\ \mathbf{y}]^T(\mathbf{P_m} + \mathbf{n}) - \mathbf{s_k}|^2 < |\,[\mathbf{x}\ \mathbf{y}]^T\ \mathbf{n}|^2\big)$ as follows:

$$P(\widehat{k}|m) = 1 - \frac{1}{2}\,\mathrm{erfc}\left(\frac{-\mathbf{\Delta P}_{m,k}^T\,\mathbf{\Upsilon}\,\mathbf{\Delta P}_{m,k}}{2\sqrt{N_0}\sqrt{\mathbf{\Delta P}_{m,k}^T\,\mathbf{\Upsilon}^2\,\mathbf{\Delta P}_{m,k}}}\right) \tag{8}$$

where $\mathbf{s_k} = [\mathbf{x}\ \mathbf{y}]^T\ \mathbf{P_k}$, $\boldsymbol{\Upsilon} \equiv [\mathbf{x}\ \mathbf{y}]\,[\mathbf{x}\ \mathbf{y}]^T$, $\boldsymbol{\Delta}\mathbf{P}_{m,k} \equiv \mathbf{P_m} - \mathbf{P_k}$ and erfc is the complementary error function. Probability of bit error denoted by P_e^b is approximately equal to $P_e^s\ /\ M$.

CHAPTER VIII

NUMERICAL CALCULATIONS

Numerical calculations and performance parameters of the hybrid system are explained in two sections such as downlink and uplink at below.

Capacity per house, K, LED unit and N_h for clear sky simulation results are shown in Fig. 21, 23, 24, 25. In Fig. 22, 26, 27 capacity for each LED with $f_{eff} = 1000$ mm, $V = 20$ km and $D_{LED} = 20$ mm for varying P_T, and capacity per house with $f_{eff} = 1000$ mm and $P_{Tot}^{T} = 100$ W for varying D_{LED} ($V = 20$ km) and fog level are simulated for uplink side.

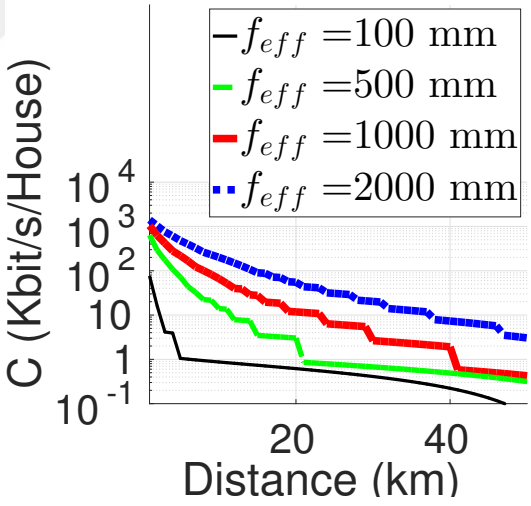

Figure 21. Capacity per house for clear sky with $V = 20$ km, $D_{LED} = 20$ mm and $P_{Tot}^{T} = 100$ W.

In the downlik side, IM capacity performance of VLC channels utilizing LCD and QD, and OLED display screens for varying SNR and k_I in Fig. 28. In addition, P_e^b for varying $E_b \,/\, N_0$ and modulation orders with 4-CSK, 8-CSK and 16-CSK for QD, OLED, LCD are simulated in Fig. 29.

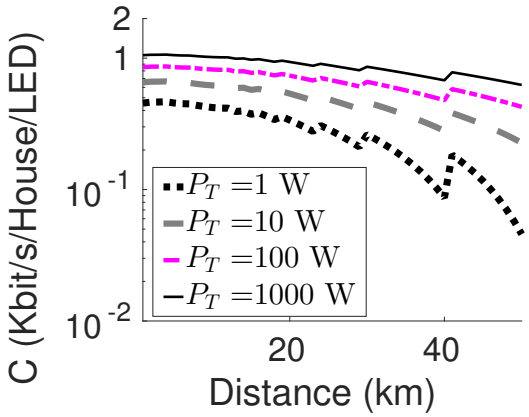

Figure 22. Performance with respect to d showing capacity for each LED with f_{eff} = 1000 mm, V = 20 km and D_{LED} = 20 mm for varying P_T.

8.1 Uplink Performance

TABLE VI. Uplink performance parameters.

PARAMETER	VALUES	PARAMETER	VALUES
f_{eff}	100 mm - 2000 mm	d_h	10 m
D_{LED}	1 mm - 200 mm	s	5.2 μ m
W_{LED}	1 m	w_s	5.4 mm
P_T^{Tot}	1 W - 1000 W	$\Phi_{1/2}$	60°
P_n	600 mW/cm^2	φ	0°
A	f_{eff} / 10	n	1.5
λ	650 nm	R_p	0.5 A/W
V	0.5 km - 20 km	$T_s(\phi)$	1
d	1 km - 50 km		

Uplink performance is numerically calculated for the parameters defined in Table VI. f_{eff} is chosen in the interval (100 mm - 2000 mm) achieving long range communications. Total area of the LED array, i.e., W_{LED}, is chosen as one square meter as a practical size to be deployed on the roofs of the houses. The color is chosen as red with wavelength 650 nm, however, other colors can also be experimented in terms of performance. Aperture size is chosen as f_{eff} / 10 as a medium level ratio reaching

both short and long range capabilities. The distance between homes is assumed as $d_h = 10$ m. Furthermore, sensor pixel (s) and array size (w_s) are chosen similar to practical camera based receiver architectures, e.g., [33]. Noise power spectral density is taken as the same with experimental results of machine vision based cameras in [33]. The semiangle $\Phi_{1/2}$ is chosen as 60°, φ as zero for simplicity, $n = 1.5$, $T_s(\phi)$ as one and R_p as 0.5 A/W in accordance with similar simulations studies in [6, 33].

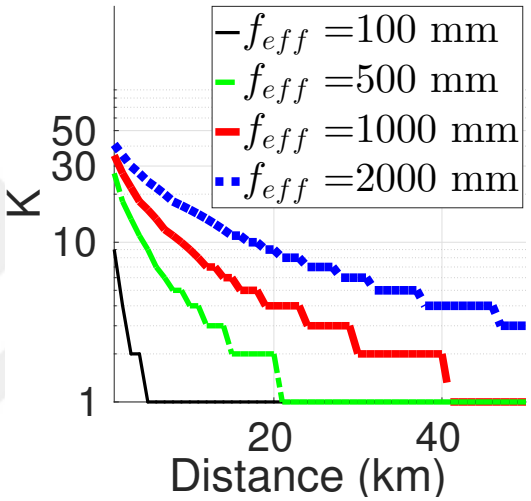

Figure 23. K for clear sky with $V = 20$ km, $D_{LED} = 20$ mm and $P_{Tot}^{T} = 100$ W.

In Figs. 21, 23, 24 and 25 capacity per house, K, capacity per single LED unit in each house and N_h are shown, respectively, for clear sky with $V = 20$ km, $D_{LED} = 20$ mm and the total transmission power of the array being equal to $P_T^{Tot} = 100$ W chosen less than the power consumption of a high power commercial LED bulb. The performances are calculated for varying focal lengths of the telescope. In Fig. 21, it is shown that the uplink capacity for each house extends from hundreds of bits to thousands of Kbps for coverage distance reaching $d = 50$ km.

Focal length increases the total capacity due to the increased resolution allowing to detect more individual LEDs on the arrays of each house as shown in Fig. 23. Each LED experiences higher capacity with short focal length until $d \approx 10$ km while different focal lengths result in the same performance for d in $\approx$ (10-40) km as shown

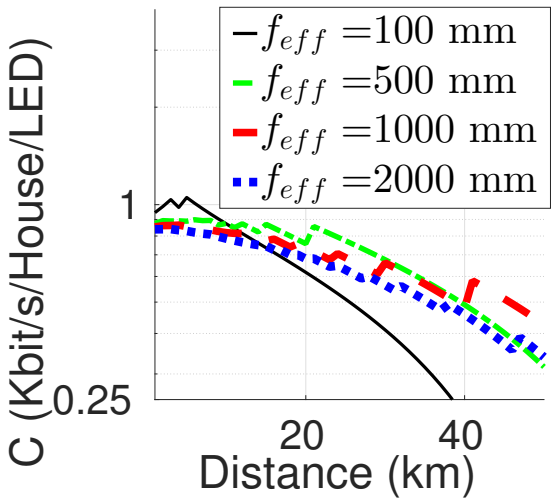

Figure 24. Capacity per LED unit for clear sky with $V = 20$ km, $D_{LED} = 20$ mm and $P_{Tot}^{T} = 100$ W.

in Fig. 24.

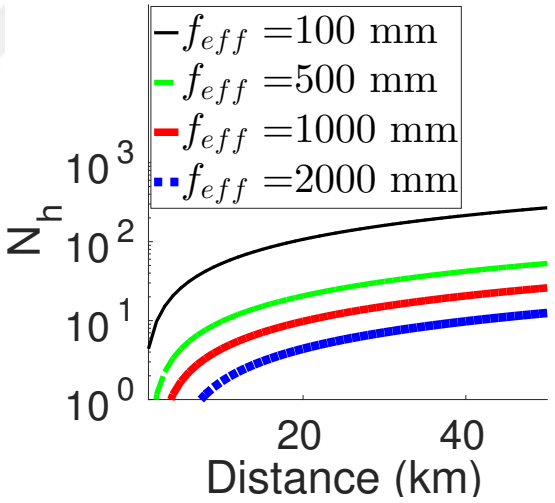

Figure 25. N_h for clear sky with $V = 20$ km, $D_{LED} = 20$ mm and $P_{Tot}^{T} = 100$ W.

In higher ranges, $f_{eff} = 1000$ nm provides better capacity for each individual LED unit. On the other hand, the number of served houses by each telescope increases with shorter focal length and higher distance as shown in Fig. 25. Therefore, there is a trade-off among capacity per house, N_h and d as shown in Figs. 21 and 23.

In Fig. 22, it is observed that higher power above 100 W allows data rates reaching Kbps at tens of kilometers distance for each LED unit.

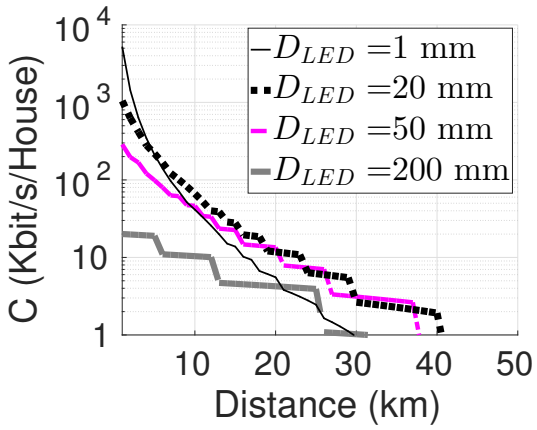

Figure 26. Capacity per house with $f_{eff} = 1000$ mm and $P_{Tot}^{T} = 100$ W for varying D_{LED} ($V = 20$ km).

LED diameter of 20 mm provides good performance at both short and long ranges as shown in Fig. 26. Furthermore, fog level majorly reduces the capacity as shown in Fig. 27 as a challenging issue to be solved for long range VLC communications.

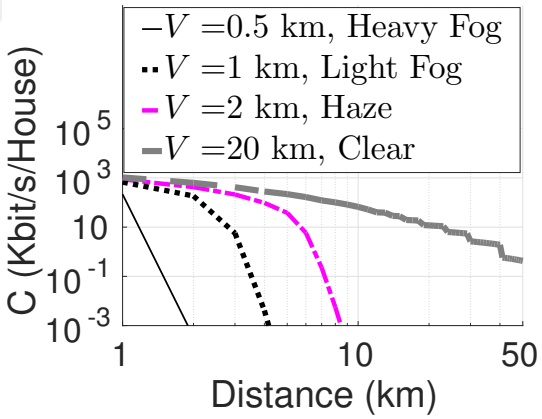

Figure 27. Capacity per house with $f_{eff} = 1000$ mm and $P_{Tot}^{T} = 100$ W for varying fog level.

8.2 Downlink Performance

The capacity performances are compared by assuming full HD resolution, i.e., $W_{px} = 1920 \times 1080$. IM capacity performance comparison of LCD and QD is shown in Fig. 28(a) while the performance for OLED is shown in Fig. 28(b). W_r is chosen as 1000 Hz for LCD and QD, and 100 KHz for OLED to analyze the best performances

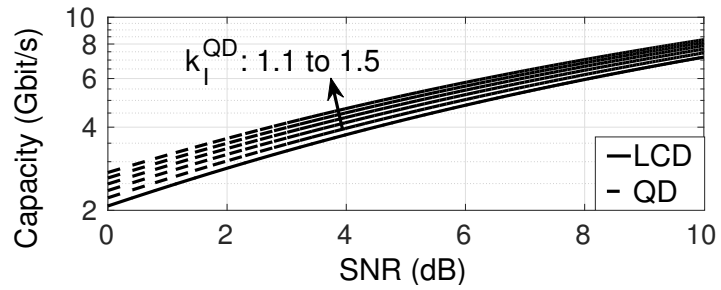

(a)

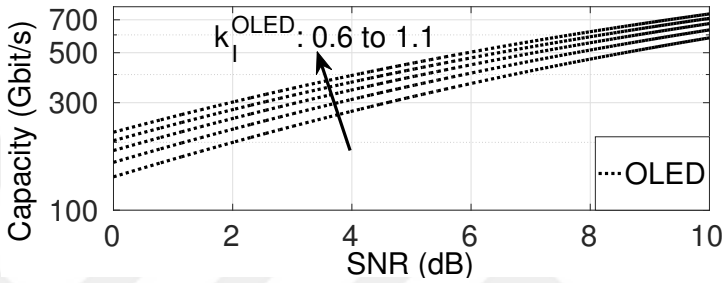

(b)

Figure 28. IM capacity performance of VLC channels utilizing (a) LCD and QD, and (b) OLED display screens for varying SNR and k_I.

achievable with the state-of-the-art technology. Power efficiency factor of QD, i.e., k_I^{QD}, is simulated for varying values from 1.1 to 1.5 as observed in [11]. SNR for each receiver pixel is simulated for varying levels of noise from 0 to 10 dB. It is observed in Fig. 28(a) that QD and LCD have comparable capacity performances while QD performance increases significantly at low SNR regime as the power efficiency increases. Therefore, QD is preferred for VLC purposes at low SNR condition. On the other hand, power efficiency factor of OLED is chosen between $k_I^{OLED} = 0.6$ to 1.1 to account for the fact that varying levels of efficiencies are observed in literature compared with LCD, e.g., observing 60 lm/W and 100 lm/W efficiencies for OLEDs and LEDs, respectively, and 10% more efficient OLED TVs compared with LCD TVs [15]. However, OLED screen has significantly higher capacity, i.e., approximately fifty times higher compared with QD and LCD displays, due to lower response time and higher frame rate of 100 KHz. Therefore, OLED TVs have the potential to allow Tbit/s data communication rates in a perfect MIMO communication architecture.

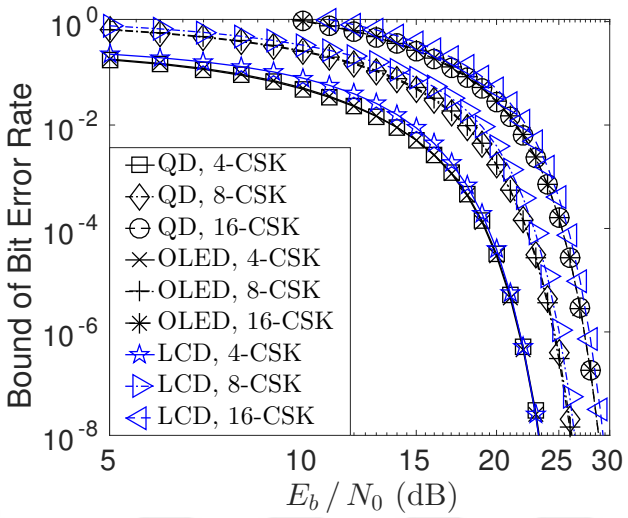

Figure 29. Bound on P_e^b for varying $E_b\,/\,N_0$ and modulation orders with 4-CSK, 8-CSK and 16-CSK.

CSK performances of TVs are compared in terms of the bound on the probability of bit error in Fig. 29. P_e^b performance is simulated for varying $E_b\,/\,N_0$. E_b is given by $1/M$ (W) if it is assumed that the symbol power is chosen as 1 W. M-CSK performances are simulated for constellation order M being equal to 4, 8 and 16. Optimized three dimensional (3D) constellation set defined in [48] is utilized to calculate $\mathbf{P}_m$ for mth symbol. It is observed in Fig. 29 that OLED and QD display screens have better error performances due to increased CG compared with LCD screens such that the minimum distance between the symbols increases. The improvement in error performance is more easily observed at high SNR regime. As a result, OLED and QD based screen technologies are future promising for both more reliable VLC performance and higher order modulation architectures.

In addition, QD display screens have narrow spectral output as shown in Fig. 11 such that the interference between different symbols is lower and higher inter-symbol distance is achieved for a fixed symbol power compared with OLED and LCD technologies.

TABLE VII. Cost analysis for each component of the proposed ISP system.

Type	Model	Reference	Price ($)	Feature
Telescope	Meade Lx70-Eq	[50]	1386	Focal length: 1000 mm
Telescope	Bresser N-203	[51]	1263	Focal length: 1000 mm
Telescope	Celestron 6SE	[52]	1738	Focal length: 1500 mm
Telescope	Meade LS-8	[53]	4533	Focal length: 2000 mm
Camera	Basler scA640	[54]	426	Pixel size: 5.6 μ m
LED array	High power LED	[55]	192	Power: 100 W, Array size : 4 x 4
LED array	High power LED	[55]	768	Power: 100 W, Array size : 16 x 16

CHAPTER IX

OVERALL SYSTEM COST ANALYSIS AND CHALLENGES

In this chapter, estimated cost of overall system is summarized including telescopes, CCD cameras, LED arrays, Tx and Rx circuits. Firstly, each component is analysed seperately. Then, overall system cost value is calculated.

9.1 Telescope Cost Analysis

In this thesis, we utilize maximum 2000 mm focal length telescopes. The focal length of 1000 mm provides better capacity for each individual LED unit in higher ranges up to 50 km.

9.2 CCD Camera Cost Analysis

In Table VII, a CCD camera price is written based on practical camera based receiver architectures [33].

9.3 LED Array Cost Analysis

The total estimated cost of 100 W 4 x 4 and 8 x 8 LED arrays are listed in Table VII.

TABLE VIII. System components and total minimum cost calculations for one house and one cell.

	Components	Cost ($)
Cost for one house	4 x 4 LED array, indoor Tx and Rx circuit	342
Cost for one cell (ISP)	Bresser N-203 1000 mm telescope (1 pc), Basler scA640 CCD camera (1 pc)	1689

9.4 Indoor Uplink Tx and Rx Unit Cost Analysis

The total cost of indoor uplink unit including VLC Tx circuit driving LEDs and VLC Rx circuit is expected to be 150 USD [56].

9.5 Total Minimum Cost Value

The minimum system cost of one house is expected to be at least 342 USD including a LED array and indoor Tx and Rx circuit. The cost of one cell (ISP) comprising a 1000 mm focal length telescope and a CCD camera is to be around 1689 USD. These cost calculations are based on reference estimated values in Table VIII.

CHAPTER X

CHALLENGES AND FUTURE WORK

There is a set of challenges and future research issues making the hybrid system more practical. Multi-user encoding architecture storing data of multiple users in the form of TV broadcast images is needed for downlink part of the system. Synchronization is essential among TV broadcast station, uplink camera-telescope receiver and VLC indoor TX-RX units with reasonable latency and delay. Data link and MAC layer protocols design is needed achieving the proper hybrid communication. For our system, assignment of unique TV channels for ISP purposes needed. A low cost indoor VLC TX-RX unit design is a huge step for overall cost efficiency. In addition, testing low cost combinations of multiple camera and telescope units in a highly fixed positioning and orientation in real life is one of the most important future work. Mobile phone high frame rate camera receiver design is needed to fully utilize OLED TV display transmitters. Besides, analysis of the effects of spectral distribution of RGB colors on CSK performance for each display type and constellation design utilizing infinite contrast ratio of OLED screen are challenging issues. Experimental studies modeling the effects of fog and flying insects on the overall system performance are interesting and useful to realize the hybrid system in real life scnearios in rural areas.

CHAPTER XI

CONCLUSION

In this thesis, a hybrid TV RF broadcast and VLC cellular communications infrastructure model is proposed for ISP infrastructures in developing regions. VLC based outdoor uplink and indoor downlink capacities are theoretically modeled and numerically simulated including severe outdoor attenuation due to fog. The performances of QD, OLED and LCD display screen indoor transmitters are theoretically analyzed and compared in terms of channel capacity, probability of error, response time, CG, spectral color output, contrast ratio, power consumption and lifetime on VLC performance. It is shown that uplink capacity with a single high focal length telescope and ordinary digital camera receiver reaches hundreds of Kbps data rates at tens of kms distances and with coverage areas including hundreds of houses by using a LED array of one square meter area and less than hundred watts power consumption at each house. Indoor downlink synchronized with TV broadcast promises several Mbps data rate for each house.

Bibliography

[1] S. Wu, H. Wang and C.H. Youn, "Visible Light Communications for 5G wireless networking systems: from fixed to mobile communications," *IEEE Network*, vol. 28, no. 6, pp. 41–45, 2014.

[2] A. M. Cailean and M. Dimian, "Toward environmental-adaptive Visible Light Communications receivers for automotive applications: A Review", *IEEE Sensors Journal*, vol. 16, no. 9, pp. 2803-2811, 2016.

[3] Y. Wang et al., "Long-range high-speed Visible Light Communication system over 100-m outdoor transmission utilizing receiver diversity technology", *Optical Engineering*, vol. 55, no. 5, pp. 056104–056104, 2016.

[4] I. Takai, S. Ito, K. Yasutomi, K. Kagawa, M. Andoh, and S. Kawahito, "LED and CMOS image sensor based optical wireless communication system for automotive applications," *IEEE Photon. J.*, vol. 5, no. 5, 2013, Art. ID 6801418.

[5] R. Corsini et al., "Free space optical communication in the visible bandwidth for V2V safety critical protocols," *Proc. of The 8th Int. Conf. Wireless Commu. Mobile Comput. (IWCMC)*, pp. 1097–1102, 2012.

[6] H. J. Kim, A. Sewaiwar and Y. H. Chung, "Maritime Visible Light Communication with sea spectrum models", *International Journal of Communications*, vol. 9, pp. 73–76, 2015.

[7] Z. Minglun, Z. Peng and J. Yinjie, "A 5.7 Km Visible Light Communications experiment demonstration", *Proc. of The IEEE Seventh International Conference on Ubiquitous and Future Networks*, pp. 58–60, 2015.

[8] Irina Stefan and Harald Haas, "Hybrid visible light and radio frequency communication systems," *Proc. of The IEEE 80th Vehicular Technology Conference*, pp.1-5, 2014

[9] P.H. Pathak et al., "Visible Light Communication, networking, and sensing: A survey, potential and challenges," *IEEE Communications Surveys & Tutorials*, vol. 17, no. 4, pp. 2047–2077, 2015.

[10] Y. H. Kim, W. A. Cahyadi and Y. H. Chung), "Experimental demonstration of VLC-based vehicle-to-vehicle communications under fog conditions", *IEEE Photonics Journal*, vol. 7, no. 6, pp. 1–9, 2015.

[11] J. V. Derlofske et al., "Quantum dot enhancement of color for LCD Systems," *White Paper, 3M Company, USA*, 2013.

[12] J. Chen, V. Hardev and J. Yurek, "Quantum-dot displays: Giving LCDs a competitive edge through color," *Information Display*, vol. 1, no. 13, pp. 1–7, 2013.

[13] A. Kar and A. Kar, "New generation illumination engineering - an overview of recent trends in science & technology," *Proc. of The IEEE First International Conference on Automation, Control, Energy and Systems (ACES)*, pp. 1–6, 2014.

[14] Z. Luo, D. Xu and S. T. Wu, "Emerging Quantum-dots-enhanced LCDs," *Journal of Display Technology*, vol. 10, no. 7, pp. 526-539, 2014.

[15] W. Y. Park, A. Phadke, N. Shah, and V. Letschert, "TV energy consumption trends and energy-efficiency improvement options," *Ernest Orlando Lawrence Berkeley National Laboratory*, LBNL-5024E, 2011.

[16] K. Marrin, "Quantum dot display technology processes ship in LED-backlight LCD TVs," *LEDs Magazine*, vol. 10, no. 12, December 2013.

[17] R. Mertens, "The OLED Handbook," *lulu.com*, 2015.

[18] R. Zhu et al., "Realizing Rec. 2020 Color Gamut with Quantum Dot Displays," *Optics Express*, vol. 23, no. 18, pp. 23680–23693, 2015.

[19] P. Boher et al., "Optical characterization of OLED displays," *Journal of the Society for Information Display*, vol. 23, no. 9, pp. 429–437, 2015.

[20] G. Sharma, "LCDs versus CRTs-color-calibration and gamut considerations," *Proceedings of the IEEE*, vol. 90, no. 4, pp. 605-622, 2002.

[21] X Company, "Balloon-powered internet for everyone" Internet: www.x.company/loon/technology, [Nov. 16, 2017]

[22] T. S. Perry. "Aquila drone creates a laser-net in the sky." Internet: www.spectrum.ieee.org/view-from-the-valley/robotics/drones/facebooks-aquila-drone-creates-a-lasernet-in-the-sky, Apr. 13, 2016 [Nov. 15, 2017].

[23] M. B. Rahaim, A. M. Vegni, and T. D. C. Little, "A hybrid radio frequency and broadcast visible light communication system," *Proc. of The IEEE GC Wkshps*, Houston, TX, USA, pp. 792796, 2011.

[24] H. Chowdhury, I. Ashraf, and M. Katz, "Energy-efficient connectivity in hybrid radio-optical wireless systems," *Proc. of The 10th ISWCS*, Berlin, Germany, pp. 15, 2013.

[25] X. Bao, X. Zhu, T. Song, and Y. Ou, "Protocol design and capacity analysis in hybrid network of Visible Light Communication and OFDMA systems", *IEEE Transactions on Vehicular Technology*, vol. 63, no. 4, May 2014.

[26] H. Ma, L. Lampe, and S. Hranilovic, "Hybrid Visible Light and Power Line Communication for indoor multiuser downlink," *Journal of Optical Communications and Networking*, vol. 9, August 2017.

[27] T. Komine and M. Nakagawa, "Integrated system of White LED Visible Light Communication and Power-Line Communication, *IEEE Transactions Consumer Electronics*, vol. 49, pp. 7179, 2003.

[28] M. T. Alresheedi, A. T. Hussein, J. M.H. Elmirghani, "Uplink design in VLC systems with IR sources and beam steering ISSN," *IET Communications*, vol. 11, pp. 311317, 2017.

[29] M. T. Alresheedi, A. T. Hussein, and J. M. H. Elmirghani "Hybrid Diffuse IR transmitter supporting VLC systems with imaging receivers," *Proc. of The ICTON*, pp.1-6, 2016

[30] Rocketmime, "Telescope Equations." Internet: http://www.rocketmime.com/astronomy /Telescope/ResolvingPower.html, November 16, 2012 [November 8, 2016]

[31] G. Y. Hu, C. Y. Chen and Z. Q. Chen, "Free-Space Optical communication using visible light", *Journal of Zhejiang University SCIENCE A*, vol. 8, no. 2, pp.186–191, 2007.

[32] Z. Minglun, Z. Peng and J. Yinjie, "A 5.7 Km Visible Light Communications experiment demonstration", *Proc. of The IEEE Seventh International Conference on Ubiquitous and Future Networks*, pp. 58–60, 2015.

[33] A. Ashok, M. Gruteser, N. Mandayam and K. Dana, "Characterizing multiplexing and diversity in Visual MIMO", *Proc. of The IEEE 45th Annual Conference on Information Sciences and Systems (CISS)*, pp. 1–6, 2011.

[34] R. Monnier, J. B. Rault and T. de Couasnon, "Digital television broadcasting with high spectral efficiency [Modern design]", *International Broadcasting Convention*, pp. 380–384, 1992.

[35] S. Hranilovic and F. R. Kschischang, "A Pixelated MIMO wireless optical communication system," *IEEE Journal of Selected Topics in Quantum Electronics*, vol. 12, no. 4, pp. 859–874, 2006.

[36] A. Ashok et al., "Capacity of pervasive camera based communication under perspective distortions," *Proc. of The IEEE International Conference on Pervasive Computing and Communications*, pp. 112–120, 2014.

[37] R. Kays, "Modulation concepts for Visible Light Communication using video displays," *IEEE 5th International Conference on Consumer Electronics Berlin (ICCE-Berlin)*, pp. 388-392, 2015.

[38] T. Li et al., "Hilight: Hiding Bits in Pixel Translucency Changes," *ACM SIGMOBILE Mobile Computing and Communications Review*, vol. 18, no. 3, pp. 62–70, 2015.

[39] L. U. Khan, "Visible Light Communication: Applications, architecture, standardization and research challenges," *Elsevier, Digital Communications and Networks 3 (2017)*, pp.78-88, 2017

[40] T. Hao, R. Zhou and G. Xing, "COBRA: Color Barcode Streaming for Smartphone Systems," *Proc. of the 10th ACM International conference on Mobile systems, applications, and services*, pp. 85–98, 2012.

[41] A. Wang et al., "Inframe: Multiflexing Full-frame Visible Communication Channel for Humans and Devices," *Proc. of the 13th ACM Workshop on Hot Topics in Networks*, pp. 23:1–23:7, 2014.

[42] S. D. Perli, N. Ahmed and D. Katabi, "Pixnet: Interference-free Wireless Links Using LCD-camera Pairs," *Proc. of The 16th Annual International Conference on Mobile Computing and Networking*, pp. 137–148, 2010.

[43] J. M. Kahn and J. R. Barry, "Wireless infrared communications", *Proceedings of the IEEE*, vol. 85, no. 2, pp. 265–298, 1997.

[44] J. G. Proakis, "Digital Communications," *McGraw-Hill*, New York, 1995.

[45] R. Singh, T. OFarrell and J. P. David, "Performance evaluation of IEEE 802.15.7 CSK physical layer," *Proc. of The IEEE Globecom Workshops*, pp. 1064–1069, 2013.

[46] R. Singh, T. OFarrell and J. P. David, "An enhanced Color Shift Keying modulation scheme for high-speed wireless Visible Light Communications," *Journal of Lightwave Technology*, vol. 32, no. 14, pp. 2582–2592, 2014.

[47] D. M. Hoffman, N. N. Stepien and W. Xiong, "The importance of native panel contrast and local dimming density on perceived image quality of high dynamic range displays," *Journal of the Society for Information Display*, vol. 24, no. 4, pp. 216–228, 2016.

[48] J. M. Luna-Rivera et al., "Multiuser CSK scheme for Indoor Visible Light Communications," *Optics Express*, vol. 22, no. 20, pp. 24256–24267, 2014.

[49] D. Karunatilaka, F. Zafar, V. Kalavally, " LED based Indoor Visible Light Communications: State of the Art," *IEEE Communication Surveys and Tutorials*, vol. 17, no. 3, 2015.

[50] Hepsiburada, "Meade 5" L x 70 - Eq (120 / 1000 mm) Telescope" Internet: http://www.hepsiburada.com/ara?q=Meade+5, [Jan. 02, 2018]

[51] Tekzen, "Bresser Messier N - 203 (203 / 1000 mm) Telescope." Internet: http://www.tekzen.com.tr/ara?q=Bresser+Messier+N-203+, [Jan. 02, 2018]

[52] Hepsiburada, "Celestron NexStar 6SE PRO Telescope 1500 mm." Internet: http://www.hepsiburada.com, [Jan. 02, 2018]

[53] Hizlial, “Meade 8” LS - 8 (203 / 2000 mm) Telescope.” Internet: https://www.hizlial.com, [Jan. 02, 2018]

[54] Ebay, “Basler Scout scA640 - 120 fm Area Scan Camera.” Internet: https://www.ebay.com/itm/BASLER-SCOUT-scA640-120fm-AREA-SCAN-CAMERA-PENTAX-TV-LENS-25mm-C2514-M, [Jan. 02, 2018]

[55] Alibaba, “100 W High Power LED.” Internet: https://www.alibaba.com, [Jan. 03, 2018]

[56] R. D. Lab, “VLC Tx and Rx Kit.” Internet: https://researchdesignlab.com/lifi-communication-diy-kit-pic.html, [Jan. 03, 2018]

VITA

Sezgin ŞENCAN is born in 1990, in İstanbul, Turkey. He has received his B.Sc degree from Electrical and Electronics Engineering Department of Ege University in 2013. He has been working at VESTEL as Application Specialist since 2013. His current research interests are visible light communications, new display technologies, wireless optical communication systems.